

## Journal Pre-proofs

Two novel classes of fused azaisocytosine-containing congeners as promising drug candidates: Design, synthesis as well as *in vitro*, *ex vivo* and *in silico* studies

Małgorzata Sztanke, Jolanta Rzymowska, Małgorzata Janicka, Krzysztof Sztanke

PII: S0045-2068(19)30556-5  
DOI: <https://doi.org/10.1016/j.bioorg.2019.103480>  
Reference: YBIOO 103480

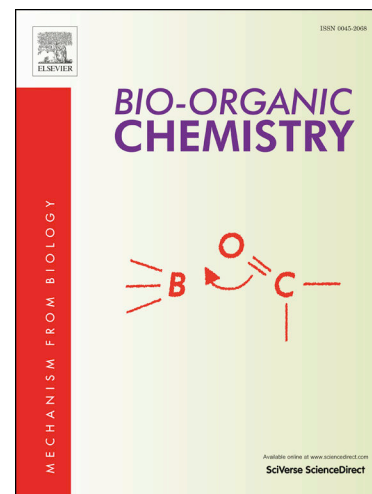
To appear in: *Bioorganic Chemistry*

Received Date: 10 April 2019  
Revised Date: 23 November 2019  
Accepted Date: 25 November 2019

Please cite this article as: M. Sztanke, J. Rzymowska, M. Janicka, K. Sztanke, Two novel classes of fused azaisocytosine-containing congeners as promising drug candidates: Design, synthesis as well as *in vitro*, *ex vivo* and *in silico* studies, *Bioorganic Chemistry* (2019), doi: <https://doi.org/10.1016/j.bioorg.2019.103480>

This is a PDF file of an article that has undergone enhancements after acceptance, such as the addition of a cover page and metadata, and formatting for readability, but it is not yet the definitive version of record. This version will undergo additional copyediting, typesetting and review before it is published in its final form, but we are providing this version to give early visibility of the article. Please note that, during the production process, errors may be discovered which could affect the content, and all legal disclaimers that apply to the journal pertain.

© 2019 Published by Elsevier Inc.



**Two novel classes of fused azaisocytosine-containing congeners as promising drug candidates: design, synthesis as well as *in vitro*, *ex vivo* and *in silico* studies**

**Małgorzata Sztanke<sup>a\*</sup>, Jolanta Rzymowska<sup>b</sup>, Małgorzata Janicka<sup>c</sup>, Krzysztof Sztanke<sup>d</sup>**

<sup>a</sup>Chair and Department of Medical Chemistry, Medical University, 4A Chodźki Street, 20-093 Lublin, Poland

<sup>b</sup>Department of Biology and Genetics, Medical University, 4A Chodźki Street, 20-093 Lublin, Poland

<sup>c</sup>Department of Physical Chemistry, Faculty of Chemistry, Maria Curie-Skłodowska University, Maria Curie-Skłodowska Sq. 3, 20-031 Lublin, Poland

<sup>d</sup>Laboratory of Bioorganic Synthesis and Analysis, Chair and Department of Medical Chemistry, Medical University, 4A Chodźki Street, 20-093 Lublin, Poland

\* Corresponding author. Tel.: +48-81-4486195

e-mail address: malgorzata.sztanke@umlub.pl (M. Sztanke)

**Abstract**

Searching for new less toxic anticancer drug candidates is a big challenge from a medical point of view. The present investigation was aimed at describing two independent synthetic approaches based on isosteric replacements, spectroscopic characteristics, *in vitro* anticancer and *ex vivo* antihaemolytic activities of novel molecules (**9-22**) and correlations between their standardised lipophilicity indices, computed  $\log P_{\text{average}}$  values and pharmacokinetic descriptors. Two novel protocols for annelation of the triazinone template on hydrazinylideneimidazolidines (**1-8**) (showing a high reactivity towards electrophilic reagents, such as ethyl trifluoropyruvate and ethyl 3-methyl-2-oxobutyrate) were developed for the first time, giving rise to two original classes of highly conjugated azaisocytosine-containing molecules (**9-16** and **17-22**). Both syntheses proceeded under basic conditions to yield the most probable intermediates (*e.g.* hemiaminals and imines), which in refluxing two-component solvent mixtures or a suitable solvent cyclised through closing the triazinone ring on functionalised imidazolidines in both cases. All fused azaisocytosine-containing congeners were investigated with the purpose of preselecting possible drug candidates with a better selectivity that could be suitable for further more detailed drug development studies. The majority of test molecules revealed strong antiproliferative effects in most tumour cell cultures and they were more cytotoxic against tumour cells than anticancer drug – pemetrexed. These cytotoxicities may be associated with the activation of initiator and executioner caspases (confirmed for compound **12**) which are inducers of apoptosis. Simultaneously, three bioisosteres bearing the trifluoromethyl moiety at the *C*-3 and the *ortho* substitution at the phenyl ring (**10**, **12** and **13**) proved to be the most promising in terms of selectivity as they were less or equally toxic to normal cells as pemetrexed. It was shown that isosteric replacement of the ethyl group in antitumour active congeners by the trifluoromethyl or isopropyl group was favourable for the selectivity of the designed drug-like molecules. Almost all new compounds revealed the protective effects in an *ex vivo* model of oxidatively stressed rat erythrocytes (better or comparable than that of ascorbic acid/Trolox), proving that they are safe to red blood cells. The statistically significant and predictive QSAR equations were derived that describe relationships between some pharmacokinetic descriptors (such as  $\log K_a$ ,  $HSA$ ,  $f_{u, \text{brain}}$ , Caco-2,  $\log K_p$ ) and lipophilicity parameters of test molecules. Among all molecules with anticancer profile, the possible drug candidates seem to be **10**, **12**, **13**, **19** and **21** which are the least toxic for normal cells, deprived of haemolytic effects on oxidatively-stressed red blood cells and have the optimum pharmacokinetic descriptors in terms of their lipophilicity parameters. Because of a high development potential they should be utilised in

further more extended *in vivo* investigations aimed at developing novel less toxic anticancer agents.

**Keywords**

Drug candidates

Azaisocytosine-containing bioisosteres

Bioisosteric replacements

*In vitro* anticancer activity

*Ex vivo* oxidative haemolysis inhibition

*In silico* pharmacokinetic descriptors

QSAR

Journal Pre-proofs

## 1. Introduction

Bioisosteres of cytosine and cytidine, containing the *s*-triazinone scaffold (such as azacytosine and the clinically useful 5-azacytidine), have been obtained by the isosteric replacement of  $-\text{CH}=\text{N}-$  in the aromatic pyrimidine ring by  $-\text{N}=\text{C}-$ . They have been shown to possess enhanced cytotoxicity towards tumour cells both *in vitro* and *in vivo* [1-3]. Notwithstanding, it has been proved that some clinically useful nucleoside and azanucleoside antimetabolites with the exocyclic amino group such as cytarabine (*e.g.* cytosine arabinoside) and 5-azacytidine, respectively, are rapidly inactivated by cytidine deaminase producing the inactive nucleoside and azanucleoside metabolites [1-3]. Therefore, these anticancer agents should not be given orally due to the high concentration of cytidine deaminase in the intestines. Considering the above-mentioned facts, the design of novel anticancer antimetabolites which are resistant to enzymatic inactivation in the gut is of great challenge from the biochemical point of view.

The persistent search for innovative antimetabolites belonging to the class of fused azaisocytosine-containing congeners (that mimic azaisocytosines) results from their high structural similarity to the canonical nucleobases, constituting the basic building blocks of nucleic acids. Such isosteric isomers of bicyclic nucleobases may be useful in future as innovative antimetabolites in cancer treatment because of three main reasons. Primary, they can act as fraudulent building blocks of nucleic acids (*e.g.* antimetabolites) during the synthesis phase and therefore inhibiting their various functions or they can interact with various enzymes that are involved in the DNA biosynthesis leading to lethal syntheses. Secondly, they cannot be inactivated by the enzyme cytidine deaminase in the gut due to the nitrogen atom of amino group locked up into an imidazolidine ring to prevent deamination [4,5]. Thirdly, a number of them should not cause a significant damage in proliferating non-tumoural cells *in vivo* in the case when they are sufficiently selective for tumour cells *in vitro* [5-14].

The structure of azaisocytosine [15] and a number of biologically important molecules incorporating the azaisocytosine template [6-8,16] has been well defined based on spectroscopic and crystallographic investigations. Two new drug-like scaffolds, such as the 7,8-dihydroimidazo[2,1-*c*][1,2,4]triazin-4(6*H*)-one and 1,2,4-triazino[4,3-*a*]benzimidazol-4(10*H*)-one, both incorporating the azaisocytosine template, have been identified as particularly useful in the rational design of novel anticancer and anti-inflammatory agents. These extremely good scaffolds have been employed successfully for designing novel

adenosine receptor antagonists being of benefit among others in cancer and inflammatory diseases including colitis [17,18] as well as for the treatment and prevention of hepatic cirrhosis [19].

Fused azaisocytosine-like molecules (**I-VI**, Fig. S1 in Supplementary material) containing 8-aryl-3-ethyl substituents at the privileged 7,8-dihydroimidazo[2,1-*c*][1,2,4]triazin-4(6*H*)-one template have been reported recently as promising innovative antimetabolite candidates with medical utility. They were more potent than pemetrexed in inhibiting the growth of three tumour (A549, HeLa, T47D) cell lines of the epithelial origin. In addition, their lipophilicity indices were correlated quantitatively with important molecular descriptors best compromising their intestinal absorption, effective permeability and blood-barrier penetration. It should be noted that of particular interest among the compounds of this class are molecules **IV** and **VI** bearing 3-chlorophenyl and 3,4-dichlorophenyl substitution, respectively, at the *N*-8 of the privileged scaffold. They have been shown to produce significantly lower cytotoxic effects in non-tumoural cells of the same epithelial origin [5]. Besides, all the molecules (**I-VI**) belonging to this class with selectivity indices better or comparable to anticancer agent – pemetrexed [5] are still under patent protection [20] as possible molecular pharmaceuticals of benefit in the treatment of human lung, cervical, breast and ovarian cancers. Notwithstanding, the 8-substituted-3-(trifluoromethyl) as well as 8-substituted-3-(propan-2-yl) counterparts bearing the privileged 7,8-dihydroimidazo[2,1-*c*][1,2,4]triazin-4(6*H*)-one template, to the best of our knowledge, have not been yet synthesised and investigated as possible anticancer agents. Taking into account the bioisosterism concept we decided to exchange the ethyl substituent in antiproliferative active fused azaisocytosine-containing congeners (Fig. S1 in Supplementary material) by the trifluoromethyl and isopropyl groups, presenting a comparable steric arrangement. The purpose of both molecular variations based on isosteric replacements of interchangeable substituents was to design novel bioisosteres with the same profile of biological activity (*e.g.* anticancer action). The subsequent issue was to analyse whether modifications resulting from isosterism are productive (leading to the enhanced antitumour activity, selectivity or the decreased toxicity) and to preselect the most promising drug-like candidates for further more advanced investigations.

The purpose of the present synthetic investigation was to elaborate, after thorough experimentation, two successful and good-yielding synthesis routes leading to the target classes of fused azaisocytosine-containing congeners. The design of these two novel classes of molecules (that are particularly different in the substitution of the trifluoromethyl or

isopropyl group at the C-3, although displaying a comparable steric arrangement to retain the profile of biological activity) was based on previously reported anticancer active 8-substituted-3-ethyl-7,8-dihydroimidazo[2,1-*c*][1,2,4]triazin-4(6*H*)-ones [5]. The subsequent challenging issue was to perform suitable modifications for entering various substituents at the N-8 allowing some structure-activity relationships to be explored with the goal of finding the optimum substitutions in both classes of the target isosteric molecules.

However, the main purpose of chromatographic investigations was to determine, for the first time, the retention-related parameters (intercepts,  $\log k_w$  and slopes, *s*), that characterise the lipophilicity scale and chromatographic behaviour of novel biologically important congeners on two different reversed-phase stationary phases (such as the endcapped octadecylsilica column and the column with immobilised artificial membrane). The subsequent aim was to employ the extrapolated lipophilicity indices ( $\log k_{w, ODS}$  and  $\log k_{w, IAM}$ ) and computed  $\log P_{average}$  values in correlation studies with relevant *in silico* pharmacokinetic descriptors (such as  $\log K_{a, HSA}$ ,  $f_{u, brain}$ , Caco-2,  $\log K_p$ ) in order to derive some quantitative structure-activity relationships (QSARs), characterising test bioisosteres with the anticipated utility in medicine.

This present paper is the continuation of our previous studies on pharmacologically important fused azaisocytosine-containing molecules of the antimetabolite-type [4,5,13,18].

## 2. Experimental protocols

### 2.1. General materials and instrumentations

Commercially available 2-oxoesters (*e.g.* ethyl dimethylpyruvate and ethyl trifluoropyruvate) of the highest grade available were purchased from Alfa Aesar (Karlsruhe, Germany). Therefore, these reagents were used without further purification. The anhydrous organic solvents for synthesis and biological studies (*e.g.* methanol – MeOH, *n*-butanol, *N,N*-dimethylformamide – DMF, dimethyl sulfoxide – DMSO) of the highest grade available were employed. Triethylamine (TEA) for synthesis from Roth (Carl Roth GmbH, Karlsruhe, Germany) was used as an alkaline substance, which binds the hydrogen iodide yielding a by-product of alkylation – triethylammonium iodide, and before use it was dried with solid KOH (distributed by POCH SA, Gliwice, Poland) and then distilled. 2,2'-Azobis(2-methylpropionamide)dihydrochloride (AAPH), hydrogen peroxide (H<sub>2</sub>O<sub>2</sub>), ascorbic acid (AA), 6-hydroxy-2,5,7,8-tetramethylchroman-2-carboxylic acid (Trolox) were supplied from

Sigma-Aldrich (Saint-Louis, MO, USA), whereas phosphate-buffered saline (PBS) – from EURx Ltd. (Gdańsk, Poland). A deionised water (Millipore quality) was also used. After completion of heterocyclisation process the volatile component/components of the reaction solution was/were evaporated to a suitable volume under reduced pressure using a rotary evaporator (Heidolph Instruments GmbH, Germany). The recrystallisation of the majority of crude solid compounds (**9-18** and **20-22**) have been carried out using the appropriate mixtures of polar protic and aprotic solvents (*e.g.* MeOH/DMF) in the proportion indicated. MeOH as a solvent was employed solely for recrystallisation of the compound **19**. All novel compounds (**9-22**) have been characterised by their physico-chemical properties (*e.g.* melting points, retention times determined on three different reversed phase columns) as well as spectroscopic data (IR, <sup>1</sup>H NMR, UV) and elemental analyses (that were consistent with the assigned structures). The melting point (m.p.) of each odourless, pure and solid compound revealed a sharp melting range (not exceeded 1°C). Each m.p. was determined using a Boetius melting point apparatus (Veb, Analytik, Dresden, Germany). The homogeneity of each compound sample was established by employing thin-layer chromatography (TLC). This preparative TLC analysis was routinely carried out at stable room temperature on commercial TLC aluminium sheets silica gel 60 F<sub>254</sub> pre-coated (Merck, Darmstadt, Germany). The obtained products were examined observing the fluorescence of their spots under UV light at  $\lambda_{\max}$  254 nm. The infrared spectra were measured on Thermo Scientific FTIR Nicolet 8700 spectrometer by means of an attenuated total reflectance (ATR) method with a diamond crystal within the spectral range 4000-400-cm<sup>-1</sup> and the spectral resolution of 4 cm<sup>-1</sup>. Each spectrum was recorded directly from the surface of a sample at room temperature and then subjected to a baseline as well as ATR correction and normalisation. The <sup>1</sup>H NMR spectra were recorded at 300 MHz on a Bruker Avance spectrometer (Germany) in two reference solvents from Merck company (Darmstadt, Germany) such as: deuterated dimethyl sulfoxide (DMSO-*d*<sub>6</sub>) – in the case of **9-16** or deuterated chloroform (CDCl<sub>3</sub>) – in the case of **17-22**. All chemical shifts are reported in ppm referenced to tetramethylsilane (TMS, Sigma-Aldrich, Saint-Louis, MO, USA) as an internal standard ( $\delta = 0$  ppm). Coupling constants (*J*) are given in hertz (Hz) with up to one digit after the decimal. The following abbreviations for the signal multiplicity were used: s – singlet, d – doublet and m – multiplet. Absorption band maxima in the ultraviolet region of electronic spectra of all the compounds (**9-22**) were determined on an U2800 Hitachi spectrophotometer (Hitachi, Tokyo, Japan). Two characteristic absorption band maxima (with extinction coefficients) of the 10% methanolic solution of each analyte are provided in the experimental section. All the performed combustion microanalyses for C,

H, Cl, F and N were agreeable within  $\pm 0.4\%$  of the theoretical values for C, H, N (in the case of **9-22**), F (in the case of **9-16**), Cl (in the case of **13-16** and **19-22**), and therefore their results were not provided in the experimental section concerning the physico-chemical and spectral characterisation of unknown compounds (**9-22**). The retention time ( $t_R$ ) of each solute was measured at 298 K (e.g. 25°C) on the cholesterol column (Cosmosil Cholester 75 x 2 mm i.d., 2.5 $\mu$ m; Genore, Nagłowice, Poland) using a mobile phase containing 50% (v/v) acetonitrile – MeCN (Merck, Darmstadt, Germany) in the buffer adjusted to pH 7.4 as well as on the endcapped octadecyl silica (ODS) column (Hypersil 4.0 x 125 mm;  $d_p = 5\mu$ m; Merck, Darmstadt, Germany) and the column with immobilised artificial membrane (IAM.P.C.DD2 100 x 4.6 mm i.d., 10  $\mu$ m; Regis Chemicals, USA) using a mobile phase containing 40% MeCN in the buffer adjusted to pH 7.4.

### 2.1.1. Synthesis of 1-substituted-2-hydrazinylideneimidazolidine hydroiodides (**1-8**)

Not commercially available 1-substituted-2-hydrazinylideneimidazolidine hydroiodides as nucleophilic centred building blocks (revealing a high reactivity towards electrophilic reagents, such as ethyl trifluoropyruvate and ethyl 3-methyl-2-oxobutyrate) were resynthesised according procedures reported in earlier papers [6,21]. A patent on the synthesis of these antibacterial agents has previously been obtained [22].

### 2.1.2. A general procedure for the synthesis of 8-substituted-3-(trifluoromethyl)-7,8-dihydroimidazo[2,1-c][1,2,4]triazin-4(6H)-ones (**9-16**) and 8-substituted-3-(propan-2-yl)-7,8-dihydroimidazo[2,1-c][1,2,4]triazin-4(6H)-ones (**17-22**)

The powdered 1-substituted-2-hydrazinylideneimidazolidine hydroiodide (0.02 mole) was suspended in 10 mL of *n*-butanol and during stirring a small molar excess of triethylamine (2.9 mL) was added dropwise. The stirring was continued and the reaction mixture was cautiously treated with ethyl trifluoropyruvate (0.02 mole) (in the case of synthesis of **9-16**) or with ethyl 3-methyl-2-oxobutyrate (0.02 mole) (in the case of preparation of **17-22**) in a dropwise manner because of exothermity of the examined reaction. The reaction mixture was allowed to stir until an intermediate solid had appeared during synthetic process of **9-16**. In turn, an intermediate appeared immediately in the stirred reaction mixture in the case of synthesis of **17-22**. Adding an appropriate amount of *n*-butanol/DMF mixture (in the case of synthesis of **9-16**) or *n*-butanol (in the case of synthesis of **17-22**), the reaction mixture was heated to its boiling point and next was refluxed with stirring until the

solid which appeared had been completely dissolved. The resulting one-phase reaction solution was still refluxed with stirring for 1-5 h (in the case of synthesis of **9-16**) or for 1-4 h (in the case of synthesis of **17-22**), examining the progress of heterocyclisation of an intermediate to the final product by TLC. Next, the reaction solution was concentrated to *ca.* half its volume after a partial evaporation of two-component solvent media (in the case of synthesis of **9-16**) or the solvent medium (in the case of synthesis of **17-22**) under reduced pressure. The resulting mixture was cooled to room temperature and then frozen until the solid began to precipitate. Then the crude product, which was formed, was filtered off, washed with distilled water (10 mL), afterwards with cold methanol (5 mL) and left to air-dry. The desiccated crude solid was then recrystallised from MeOH/DMF mixture in the proportion indicated underneath (in the case of compounds **9-18** and **20-22**) or from MeOH (in the case of **19**) to yield the desired odourless, white or creamy product in a solid state. This one was filtered off and finally dried employing a dry heat sterilizer (MOV-212S-PE, Panasonic, Japan). The following novel compounds were synthesised using this experimental protocol.

*2.1.2.1. 8-Phenyl-3-(trifluoromethyl)-7,8-dihydroimidazo[2,1-c][1,2,4]triazin-4(6H)-one (9).* Recrystallised from MeOH/DMF (3:2) mixture; yield 75%, white solid having m.p. 213-214°C. IR (ATR-FTIR) ( $\nu$ ,  $\text{cm}^{-1}$ ): 3080 (aromatic C–H stretching), 2911, 2871 (methylene C–H stretching), 1699 (C=O stretching), 1588, 1511, 1453 (aromatic skeleton stretching), 1555 (C=N stretching), 1473 (methylene C–H stretching), 1309, 1291, 1263, 1199, 1165, 1120 ( $\text{CF}_3$  stretching), 764, 693 (monosubstituted benzene ring stretching);  $^1\text{H NMR}$  ( $\delta$ , ppm,  $\text{DMSO-}d_6$ , TMS, 300 MHz): 4.14-4.29 (m, 4H,  $2\text{CH}_2$ ), 7.20-7.82 (m, 5H, aromatic–H); UV (MeOH):  $\lambda_{\text{max}}$  ( $\epsilon$ ): 255 nm (14740),  $\lambda'_{\text{max}}$  ( $\epsilon$ ): 328 nm (7440); HPLC  $_{\text{Cholesterol 298K}}$  (50% MeCN in buffer pH 7.4):  $t_{\text{R}} = 71$  s; HPLC  $_{\text{ODS 298K}}$  (40% MeCN in buffer pH 7.4):  $t_{\text{R}} = 269.2$  s; HPLC  $_{\text{IAM 298K}}$  (40% MeCN in buffer pH 7.4):  $t_{\text{R}} = 108.9$  s.

*2.1.2.2. 8-(2-Methylphenyl)-3-(trifluoromethyl)-7,8-dihydroimidazo[2,1-c][1,2,4]triazin-4(6H)-one (10).* Recrystallised from MeOH/DMF (2:1) mixture; yield 68%, white solid having m.p. 194-195°C. IR (ATR-FTIR) ( $\nu$ ,  $\text{cm}^{-1}$ ): 3073, 3058, 3034 (aromatic C–H stretching), 2975, 2949, 2910 (methyl C–H and methylene C–H stretching), 1693 (C=O stretching), 1588, 1525, 1455 (aromatic skeleton stretching), 1556 (C=N stretching), 1470, 1379 (aromatic C– $\text{CH}_3$  stretching), 1306, 1286, 1264, 1202, 1160, 1146, 1126 ( $\text{CF}_3$ ), 760 (1,2-disubstituted benzene ring stretching);  $^1\text{H NMR}$  ( $\delta$ , ppm,  $\text{DMSO-}d_6$ , TMS, 300 MHz):

2.27 (s, 3H, CH<sub>3</sub>), 4.05-4.30 (m, 4H, 2CH<sub>2</sub>), 7.29-7.45 (m, 4H, aromatic-H); UV (MeOH):  $\lambda_{\max}$  ( $\epsilon$ ): 231 nm (8320),  $\lambda'_{\max}$  ( $\epsilon$ ): 317.5 nm (5120); HPLC<sub>Cholesterol 298K</sub> (50% MeCN in buffer pH 7.4):  $t_R$  = 83 s; HPLC<sub>ODS 298K</sub> (40% MeCN in buffer pH 7.4):  $t_R$  = 242.9 s; HPLC<sub>IAM 298K</sub> (40% MeCN in buffer pH 7.4):  $t_R$  = 102.2 s.

2.1.2.3. 8-(4-Methylphenyl)-3-(trifluoromethyl)-7,8-dihydroimidazo[2,1-c][1,2,4]triazin-4(6H)-one (**11**). Recrystallised from MeOH/DMF (1:1) mixture; yield 74%, creamy solid having m.p. 267-268°C. IR (ATR-FTIR) ( $\nu$ , cm<sup>-1</sup>): 3109, 3086, 3065, 3043 (aromatic C-H stretching), 2974, 2932, 2904 (methyl C-H and methylene C-H stretching), 1702 (C=O stretching), 1584, 1510, 1483, 1455 (aromatic skeleton stretching), 1552 (C=N stretching), 1473, 1368 (aromatic C-CH<sub>3</sub> stretching), 1333, 1315, 1285, 1259, 1200, 1178, 1120 (CF<sub>3</sub> stretching), 819 (1,4-disubstituted benzene ring stretching); <sup>1</sup>H NMR ( $\delta$ , ppm, DMSO-*d*<sub>6</sub>, TMS, 300 MHz): 2.31 (s, 3H, CH<sub>3</sub>), 4.12-4.26 (m, 4H, 2CH<sub>2</sub>), 7.26 (d,  $J$  = 8.4 Hz, 2H, aromatic protons: 4-methylphenyl-H-2' and H-6'), 7.67 (d,  $J$  = 8.4 Hz, 2H, aromatic protons: 4-methylphenyl-H-3' and H-5'), UV (MeOH):  $\lambda_{\max}$  ( $\epsilon$ ): 256 nm (10100),  $\lambda'_{\max}$  ( $\epsilon$ ): 329.5 nm (4860); HPLC<sub>Cholesterol 298K</sub> (50% MeCN in buffer pH 7.4):  $t_R$  = 85.5 s; HPLC<sub>ODS 298K</sub> (40% MeCN in buffer pH 7.4):  $t_R$  = 399.7 s; HPLC<sub>IAM 298K</sub> (40% MeCN in buffer pH 7.4):  $t_R$  = 119.4 s.

2.1.2.4. 8-(2-Methoxyphenyl)-3-(trifluoromethyl)-7,8-dihydroimidazo[2,1-c][1,2,4]triazin-4(6H)-one (**12**). Recrystallised from MeOH/DMF (2:1) mixture; yield 70%, white solid having m.p. 221-222°C. IR (ATR-FTIR) ( $\nu$ , cm<sup>-1</sup>): 3072 (aromatic C-H stretching), 2941, 2904, 2840 (methylene C-H stretching and methoxy C-H stretching), 1703 (C=O stretching), 1601, 1499, 1457 (aromatic skeleton stretching), 1561 (C=N stretching), 1476 (methylene C-H stretching), 1306, 1281, 1246, 1180, 1161, 1139, 1123 (CF<sub>3</sub> stretching), 1267, 1016 (C-O-C stretching), 765 (1,2-disubstituted benzene ring stretching); <sup>1</sup>H NMR ( $\delta$ , ppm, DMSO-*d*<sub>6</sub>, TMS, 300 MHz): 3.83 (s, 3H, OCH<sub>3</sub>), 4.04-4.29 (m, 4H, 2CH<sub>2</sub>), 7.02-7.49 (m, 4H, aromatic-H); UV (MeOH):  $\lambda_{\max}$  ( $\epsilon$ ): 232 nm (10100),  $\lambda'_{\max}$  ( $\epsilon$ ): 318.5 nm (7120); HPLC<sub>Cholesterol 298K</sub> (50% MeCN in buffer pH 7.4):  $t_R$  = 68.9 s; HPLC<sub>ODS 298K</sub> (40% MeCN in buffer pH 7.4):  $t_R$  = 209.3 s; HPLC<sub>IAM 298K</sub> (40% MeCN in buffer pH 7.4):  $t_R$  = 99.4 s.

2.1.2.5. 8-(2-Chlorophenyl)-3-(trifluoromethyl)-7,8-dihydroimidazo[2,1-c][1,2,4]triazin-4(6H)-one (**13**). Recrystallised from MeOH/DMF (4:3) mixture; yield 72%, creamy solid

having m.p. 193-194°C. IR (ATR-FTIR) ( $\nu$ ,  $\text{cm}^{-1}$ ): 3094, 3067, 3029 (aromatic C–H stretching), 2904, 2838 (methylene C–H stretching), 1709 (C=O stretching), 1591, 1493, 1455 (aromatic skeleton stretching), 1561 (C=N stretching), 1472 (methylene C–H stretching), 1109 (aromatic C–Cl stretching), 1311, 1288, 1267, 1209, 1172, 1159, 1150, 1121 ( $\text{CF}_3$  stretching), 781 (1,2-disubstituted benzene ring stretching);  $^1\text{H}$  NMR ( $\delta$ , ppm,  $\text{DMSO-}d_6$ , TMS, 300 MHz): 4.09-4.35 (m, 4H,  $2\text{CH}_2$ ), 7.45-7.70 (m, 4H, aromatic–H); UV (MeOH):  $\lambda_{\text{max}}$  ( $\epsilon$ ): 230 nm (9400),  $\lambda'_{\text{max}}$  ( $\epsilon$ ): 313 nm (7500); HPLC  $\text{Cholesterol}_{298\text{K}}$  (50% MeCN in buffer pH 7.4):  $t_{\text{R}} = 64.4$  s; HPLC  $\text{ODS}_{298\text{K}}$  (40% MeCN in buffer pH 7.4):  $t_{\text{R}} = 252.7$  s; HPLC  $\text{IAM}_{298\text{K}}$  (40% MeCN in buffer pH 7.4):  $t_{\text{R}} = 106.2$  s.

*2.1.2.6. 8-(3-Chlorophenyl)-3-(trifluoromethyl)-7,8-dihydroimidazo[2,1-c][1,2,4]triazin-4(6H)-one (14)*. Recrystallised from MeOH/DMF (2:1) mixture; yield 66%, white solid having m.p. 183-184°C. IR (ATR-FTIR) ( $\nu$ ,  $\text{cm}^{-1}$ ): 3109, 3086, 3064 (aromatic C–H stretching), 2904 (methylene C–H stretching), 1702 (C=O stretching), 1597, 1576, 1504, 1456 (aromatic skeleton stretching), 1552 (C=N stretching), 1470 (methylene C–H stretching), 1110 (aromatic C–Cl stretching), 1326, 1312, 1287, 1256, 1213, 1181, 1117 ( $\text{CF}_3$  stretching), 796, 782, 681 (1,3-disubstituted benzene ring stretching);  $^1\text{H}$  NMR ( $\delta$ , ppm,  $\text{DMSO-}d_6$ , TMS, 300 MHz): 4.15-4.31 (m, 4H,  $2\text{CH}_2$ ), 7.27-8.06 (m, 4H, aromatic–H); UV (MeOH):  $\lambda_{\text{max}}$  ( $\epsilon$ ): 230 nm (13840),  $\lambda'_{\text{max}}$  ( $\epsilon$ ): 326.5 nm (3260); HPLC  $\text{Cholesterol}_{298\text{K}}$  (50% MeCN in buffer pH 7.4):  $t_{\text{R}} = 102.6$  s; HPLC  $\text{ODS}_{298\text{K}}$  (40% MeCN in buffer pH 7.4):  $t_{\text{R}} = 527.4$  s; HPLC  $\text{IAM}_{298\text{K}}$  (40% MeCN in buffer pH 7.4):  $t_{\text{R}} = 141.7$  s.

*2.1.2.7. 8-(4-Chlorophenyl)-3-(trifluoromethyl)-7,8-dihydroimidazo[2,1-c][1,2,4]triazin-4(6H)-one (15)*. Recrystallised from MeOH/DMF (2:3) mixture; yield 61%, creamy solid having m.p. 239-240°C. IR (ATR-FTIR) ( $\nu$ ,  $\text{cm}^{-1}$ ): 3107, 3088, 3012 (aromatic C–H stretching), 2908 (methylene C–H stretching), 1698 (C=O stretching), 1581, 1500, 1454 (aromatic skeleton stretching), 1553 (C=N stretching), 1476 (methylene C–H stretching), 1109 (aromatic C–Cl stretching), 1323, 1308, 1262, 1213, 1181, 1132 ( $\text{CF}_3$  stretching), 837 (1,4-disubstituted benzene ring stretching);  $^1\text{H}$  NMR ( $\delta$ , ppm,  $\text{DMSO-}d_6$ , TMS, 300 MHz): 4.15-4.29 (m, 4H,  $2\text{CH}_2$ ), 7.50-7.92 (m, 4H, aromatic–H); UV (MeOH):  $\lambda_{\text{max}}$  ( $\epsilon$ ): 259 nm (10820),  $\lambda'_{\text{max}}$  ( $\epsilon$ ): 326.5 nm (5000); HPLC  $\text{Cholesterol}_{298\text{K}}$  (50% MeCN in buffer pH 7.4):  $t_{\text{R}} = 96.2$  s; HPLC  $\text{ODS}_{298\text{K}}$  (40% MeCN in buffer pH 7.4):  $t_{\text{R}} = 509.6$  s; HPLC  $\text{IAM}_{298\text{K}}$  (40% MeCN in buffer pH 7.4):  $t_{\text{R}} = 136.5$  s.

2.1.2.8. 8-(3,4-Dichlorophenyl)-3-(trifluoromethyl)-7,8-dihydroimidazo[2,1-c][1,2,4]triazin-4(6H)-one (**16**). Recrystallised from MeOH/DMF (1:1) mixture; yield 66%, creamy solid having m.p. 210-211°C. IR (ATR-FTIR) ( $\nu$ ,  $\text{cm}^{-1}$ ): 3102, 3086, (aromatic C–H stretching), 2906 (methylene C–H stretching), 1705 (C=O stretching), 1594, 1505, 1450, (aromatic skeleton stretching), 1550 (C=N stretching), 1475 (methylene C–H stretching), 1123 (aromatic C–Cl stretching), 1098 (aromatic C–Cl stretching), 1321, 1286, 1260, 1184, 1146 ( $\text{CF}_3$  stretching), 876, 837, 710 (1,2,4-trisubstituted benzene ring stretching);  $^1\text{H}$  NMR ( $\delta$ , ppm, DMSO- $d_6$ , TMS, 300 MHz): 4.16-4.31 (m, 4H,  $2\text{CH}_2$ ), 7.68-8.20 (m, 3H, aromatic–H); UV (MeOH):  $\lambda_{\text{max}}$  ( $\epsilon$ ): 261.5 nm (6600),  $\lambda'_{\text{max}}$  ( $\epsilon$ ): 326 nm (3240); HPLC<sub>Cholesterol 298K</sub> (50% MeCN in buffer pH 7.4):  $t_{\text{R}}$  = 137 s; HPLC<sub>ODS 298K</sub> (40% MeCN in buffer pH 7.4):  $t_{\text{R}}$  = 962.9 s; HPLC<sub>IAM 298K</sub> (40% MeCN in buffer pH 7.4):  $t_{\text{R}}$  = 190.8 s.

2.1.2.9. 8-Phenyl-3-(propan-2-yl)-7,8-dihydroimidazo[2,1-c][1,2,4]triazin-4(6H)-one (**17**). Recrystallised from MeOH/DMF (3:2) mixture; yield 63%, creamy solid having m.p. 207-208°C. IR (ATR-FTIR) ( $\nu$ ,  $\text{cm}^{-1}$ ): 3078, 3012 (aromatic C–H stretching), 2930, 2869 (methylene C–H stretching and methine C–H stretching), 1683 (C=O stretching), 1587, 1515, 1496, 1448 (aromatic skeleton stretching), 1561 (C=N stretching), 1481 (methylene C–H stretching), 1375, 1366 (symmetric  $\text{CH}_3$  scissor vibrations of  $\text{CH}(\text{CH}_3)_2$ ), 759, 700 (monosubstituted benzene ring stretching);  $^1\text{H}$  NMR ( $\delta$ , ppm,  $\text{CDCl}_3$ , TMS, 300 MHz): 1.31 (d,  $J$  = 6.9 Hz, 6H,  $-\text{CH}(\text{CH}_3)_2$ ), 3.32-3.41 (m, 1H,  $-\text{CH}(\text{CH}_3)_2$ ), 4.11-4.25 (m, 4H,  $2\text{CH}_2$ ), 7.12-7.82 (m, 5H, aromatic–H); UV (MeOH):  $\lambda_{\text{max}}$  ( $\epsilon$ ): 259 nm (17760),  $\lambda'_{\text{max}}$  ( $\epsilon$ ): 315 nm (6700); HPLC<sub>Cholesterol 298K</sub> (50% MeCN in buffer pH 7.4):  $t_{\text{R}}$  = 71 s; HPLC<sub>ODS 298K</sub> (40% MeCN in buffer pH 7.4):  $t_{\text{R}}$  = 205.1 s; HPLC<sub>IAM 298K</sub> (40% MeCN in buffer pH 7.4):  $t_{\text{R}}$  = 105.7 s.

2.1.2.10. 8-(4-Methylphenyl)-3-(propan-2-yl)-7,8-dihydroimidazo[2,1-c][1,2,4]triazin-4(6H)-one (**18**). Recrystallised from MeOH/DMF (2:1) mixture; yield 68%, white solid having m.p. 203-204°C. IR (ATR-FTIR) ( $\nu$ ,  $\text{cm}^{-1}$ ): 3099 (aromatic C–H stretching), 2972, 2928, 2870 (methyl C–H stretching, methylene C–H stretching and methine C–H stretching), 1674 (C=O stretching), 1618, 1583, 1510, 1449 (aromatic skeleton stretching), 1558 (C=N stretching), 1479, 1389 (aromatic C– $\text{CH}_3$  stretching), 1379, 1370 (symmetric  $\text{CH}_3$  scissor vibrations of  $\text{CH}(\text{CH}_3)_2$ ), 803 (1,4-disubstituted benzene ring stretching);  $^1\text{H}$  NMR ( $\delta$ , ppm,  $\text{CDCl}_3$ , TMS,

300 MHz): 1.31 (d,  $J = 6.9$  Hz, 6H,  $-\text{CH}(\text{CH}_3)_2$ ), 2.32 (s, 3H,  $\text{CH}_3$ ), 3.30-3.39 (m, 1H,  $-\text{CH}(\text{CH}_3)_2$ ), 4.02-4.16 (m, 4H,  $2\text{CH}_2$ ), 7.14-7.67 (m, 4H, aromatic-H); UV (MeOH):  $\lambda_{\text{max}}$  ( $\epsilon$ ): 260.5 nm (16760),  $\lambda'_{\text{max}}$  ( $\epsilon$ ): 317 nm (5980); HPLC<sub>Cholesterol 298K</sub> (50% MeCN in buffer pH 7.4):  $t_{\text{R}} = 88$  s; HPLC<sub>ODS 298K</sub> (40% MeCN in buffer pH 7.4):  $t_{\text{R}} = 295.6$  s; HPLC<sub>IAM 298K</sub> (40% MeCN in buffer pH 7.4):  $t_{\text{R}} = 115.5$  s.

2.1.2.11. 8-(2-Chlorophenyl)-3-(propan-2-yl)-7,8-dihydroimidazo[2,1-c][1,2,4]triazin-4(6H)-one (**19**). Recrystallised from MeOH; yield 52%, white solid having m.p. 148-149°C. IR (ATR-FTIR) ( $\nu$ ,  $\text{cm}^{-1}$ ): 3084, 3068 (aromatic C-H stretching), 2934, 2870 (methylene C-H stretching and methine C-H stretching), 1686 (C=O stretching), 1576, 1513, 1446 (aromatic skeleton stretching), 1565 (C=N stretching), 1485 (methylene C-H stretching), 1387, 1368 (symmetric  $\text{CH}_3$  scissor vibrations of  $\text{CH}(\text{CH}_3)_2$ ), 1089 (aromatic C-Cl stretching), 764 (1,2-disubstituted benzene ring stretching);  $^1\text{H}$  NMR ( $\delta$ , ppm,  $\text{CDCl}_3$ , TMS, 300 MHz): 1.27 (d,  $J = 6.9$  Hz, 6H,  $-\text{CH}(\text{CH}_3)_2$ ), 3.28-3.38 (m, 1H,  $-\text{CH}(\text{CH}_3)_2$ ), 4.07-4.35 (m, 4H,  $2\text{CH}_2$ ), 7.30-7.55 (m, 4H, aromatic-H); UV (MeOH):  $\lambda_{\text{max}}$  ( $\epsilon$ ): 212.5 nm (17020),  $\lambda'_{\text{max}}$  ( $\epsilon$ ): 302 nm (5280); HPLC<sub>Cholesterol 298K</sub> (50% MeCN in buffer pH 7.4):  $t_{\text{R}} = 66.5$  s; HPLC<sub>ODS 298K</sub> (40% MeCN in buffer pH 7.4):  $t_{\text{R}} = 170.1$  s; HPLC<sub>IAM 298K</sub> (40% MeCN in buffer pH 7.4):  $t_{\text{R}} = 101.5$  s.

2.1.2.12. 8-(3-Chlorophenyl)-3-(propan-2-yl)-7,8-dihydroimidazo[2,1-c][1,2,4]triazin-4(6H)-one (**20**). Recrystallised from MeOH/DMF (5:1) mixture; yield 61%, white solid having m.p. 155-156°C. IR (ATR-FTIR) ( $\nu$ ,  $\text{cm}^{-1}$ ): 3102, 3078 (aromatic C-H stretching), 2939, 2875 (methylene C-H stretching and methine C-H stretching), 1694 (C=O stretching), 1597, 1576, 1514, 1453 (aromatic skeleton stretching), 1560 (C=N stretching), 1482 (methylene C-H stretching), 1379, 1370 (symmetric  $\text{CH}_3$  scissor vibrations of  $\text{CH}(\text{CH}_3)_2$ ), 1090 (aromatic C-Cl stretching), 836, 784, 699 (1,3-disubstituted benzene ring stretching);  $^1\text{H}$  NMR ( $\delta$ , ppm,  $\text{CDCl}_3$ , TMS, 300 MHz): 1.31 (d,  $J = 6.9$  Hz, 6H,  $-\text{CH}(\text{CH}_3)_2$ ), 3.32-3.41 (m, 1H,  $-\text{CH}(\text{CH}_3)_2$ ), 4.10-4.28 (m, 4H,  $2\text{CH}_2$ ), 7.09-7.92 (m, 4H, aromatic-H); UV (MeOH):  $\lambda_{\text{max}}$  ( $\epsilon$ ): 261.5 nm (15520),  $\lambda'_{\text{max}}$  ( $\epsilon$ ): 313 nm (6540); HPLC<sub>Cholesterol 298K</sub> (50% MeCN in buffer pH 7.4):  $t_{\text{R}} = 98$  s; HPLC<sub>ODS 298K</sub> (40% MeCN in buffer pH 7.4):  $t_{\text{R}} = 428.4$  s; HPLC<sub>IAM 298K</sub> (40% MeCN in buffer pH 7.4):  $t_{\text{R}} = 138.6$  s.

2.1.2.13. 8-(4-Chlorophenyl)-3-(propan-2-yl)-7,8-dihydroimidazo[2,1-c][1,2,4]triazin-4(6H)-one (**21**). Recrystallised from MeOH/DMF (3:2) mixture; yield 59%, white solid having m.p.

209-210°C. IR (ATR-FTIR) ( $\nu$ ,  $\text{cm}^{-1}$ ): 3109, 3058 (aromatic C–H stretching), 2931, 2870 (methylene C–H stretching and methine C–H stretching), 1677 (C=O stretching), 1582, 1514, 1493, 1443 (aromatic skeleton stretching), 1557 (C=N stretching), 1475 (methylene C–H stretching), 1380, 1372 (symmetric  $\text{CH}_3$  scissor vibrations of  $\text{CH}(\text{CH}_3)_2$ ), 1097 (aromatic C–Cl stretching), 838 (1,4-disubstituted benzene ring stretching);  $^1\text{H}$  NMR ( $\delta$ , ppm,  $\text{CDCl}_3$ , TMS, 300 MHz): 1.30 (d,  $J = 6.9$  Hz, 6H,  $-\text{CH}(\text{CH}_3)_2$ ), 3.31-3.40 (m, 1H,  $-\text{CH}(\text{CH}_3)_2$ ), 4.08-4.27 (m, 4H,  $2\text{CH}_2$ ), 7.31-7.79 (m, 4H, aromatic–H); UV (MeOH):  $\lambda_{\text{max}}$  ( $\epsilon$ ): 264.5 nm (17360),  $\lambda'_{\text{max}}$  ( $\epsilon$ ): 315 nm (6460); HPLC  $_{\text{Cholesterol 298K}}$  (50% MeCN in buffer pH 7.4):  $t_{\text{R}} = 100.2$  s; HPLC  $_{\text{ODS 298K}}$  (40% MeCN in buffer pH 7.4):  $t_{\text{R}} = 393.4$  s; HPLC  $_{\text{IAM 298K}}$  (40% MeCN in buffer pH 7.4):  $t_{\text{R}} = 132.3$  s.

2.1.2.14. 8-(3,4-Dichlorophenyl)-3-(propan-2-yl)-7,8-dihydroimidazo[2,1-c][1,2,4]triazin-4(6H)-one (**22**). Recrystallised from MeOH/DMF (1:1) mixture; yield 54%, white solid having m.p. 208-209°C. IR (ATR-FTIR) ( $\nu$ ,  $\text{cm}^{-1}$ ): 3086, 3067 (aromatic C–H stretching), 2929, 2869 (methylene C–H stretching and methine C–H stretching), 1681 (C=O stretching), 1600, 1572, 1490 (aromatic skeleton stretching), 1552 (C=N stretching), 1467 (methylene C–H stretching), 1388, 1371 (symmetric  $\text{CH}_3$  scissor vibrations of  $\text{CH}(\text{CH}_3)_2$ ), 1097 (aromatic C–Cl stretching), 866, 814, 698 (1,2,4-trisubstituted benzene ring stretching);  $^1\text{H}$  NMR ( $\delta$ , ppm,  $\text{CDCl}_3$ , TMS, 300 MHz): 1.31 (d,  $J = 6.9$  Hz, 6H,  $-\text{CH}(\text{CH}_3)_2$ ), 3.33-3.42 (m, 1H,  $-\text{CH}(\text{CH}_3)_2$ ), 4.10-4.31 (m, 4H,  $2\text{CH}_2$ ), 7.41-8.02 (m, 3H, aromatic–H); UV (MeOH):  $\lambda_{\text{max}}$  ( $\epsilon$ ): 266.5 nm (5400),  $\lambda'_{\text{max}}$  ( $\epsilon$ ): 313.5 nm (2540); HPLC  $_{\text{Cholesterol 298K}}$  (50% MeCN in buffer pH 7.4):  $t_{\text{R}} = 144$  s; HPLC  $_{\text{ODS 298K}}$  (40% MeCN in buffer pH 7.4):  $t_{\text{R}} = 794.9$  s; HPLC  $_{\text{IAM 298K}}$  (40% MeCN in buffer pH 7.4):  $t_{\text{R}} = 188.7$  s.

### 2.1.3. The DNA synthesis and cellular proliferation assessment

Two classes of fused azaisocytosine-containing congeners (**9-16** and **17-22**), with the trifluoromethyl or isopropyl group attached to the C-3, respectively, and phenyl, methylphenyl, methoxyphenyl, chlorophenyl or dichlorophenyl substitution at the N-8, were subjected to investigation of their *in vitro* anticancer activities and cytotoxicities against non-cancerous cells. For this purpose, the sensitive, quantitative, reliable and relatively rapid BrdUrd-enzyme-linked immunosorbent bioassay cell-based, which is based on DNA synthesis and cell proliferation principle, was employed. The detailed procedure assessing the DNA synthesis and cellular proliferation has been reported earlier [11]. The commercially

available BrdUrd labeling and detection kit III (Roche Diagnostics GmbH, Mannheim, Germany) was used in the present study. To quantify the cellular proliferation rates (by the measure of the labeled thymidine precursor, *i.e.* 5-bromo-2'-deoxyuridine, incorporated into the DNA of proliferating cells) in tumour and non-tumoural cells (of the same epithelial origin) treated with test compounds and in untreated controls after 24-, 48- and 72-h incubation periods, the absorbance of samples was measured on a microplate reader (BIO-RAD Model 680XR, USA) at  $\lambda$  450 nm. Finally, the results derived from five independent experiments were taken and converted in order to show the growth inhibitory effects of test compounds in recruited cell cultures. Pemetrexed (Eli Lilly, Slovakia) was employed as a reference anticancer agent, which can additionally be considered as a positive control.

#### 2.1.4. Determination of caspase-6 and -8 levels in normal and cancer cells

The quantitative determination of caspase-6 and -8 levels were measured using human caspase-6 or -8 (CASP6 or CASP8) ELISA kits (SunRed Biotechnology Company, Shanghai, China). The first stage of the experiment was the preparation of reagents, standards and cell culture supernatants according to the instructions provided in the manufacturer kit. Cell lysis was performed as a result of the thermal shock from  $-186^{\circ}\text{C}$  (liquid nitrogen) to  $37^{\circ}\text{C}$  by repeating this operation three times. So prepared lysates of normal (Vero) or tumour (A549, HeLa, T47D) cells (without or with test compound **12** at a concentration of  $50\ \mu\text{g mL}^{-1}$ ) as well as biotin-(CASP5 or CASP6 or CASP8)-antibodies and Streptavidin-HRP were added to the wells that were pre-coated with Human (CASP6 or CASP8) monoclonal antibodies. Then the immune complex formed was incubated at  $37^{\circ}\text{C}$  for 60 minutes. To remove the uncombined enzyme the plate was washed five times with washing buffer. Next, chromogen solution A and chromogen solution B were added, and the incubation process was continued at  $37^{\circ}\text{C}$  for 10 minutes in the darkness. Then, to stop the reaction a stop solution was added. The optical densities (OD values) were determined within 10 minutes at  $\lambda$  405 nm using a microplate reader (BIO-RAD Model 680XR, USA). The human caspase-6 and -8 concentrations (in  $\text{ng mL}^{-1}$ ) were calculated based on the standard curve (employing standards for the individual caspases).

#### 2.1.5. Oxidative haemolysis inhibition assay

The antihaemolytic effects of fused azaisocytosine-containing congeners (**9-22**) were assessed on *ex vivo* model of erythrocytes following the procedure described earlier [13].

In order to obtain the erythrocytes the whole blood was collected from three male Wistar rats (8-9 weeks old, 200-250 g, the Experimental Medicine Centre, Lublin, Poland) and centrifuged (1000 rpm, 10 min, 4°C). After removing the plasma red blood cells were washed threefold with phosphate-buffered saline (PBS, pH 7.4) to discard erythrocytes which were lysed. Next a 4% (v/v) suspension of erythrocytes in PBS was preincubated on a water bath shaker at 37°C for 60 min with all the tested fused azaisocytosine-containing congeners (9-22) or positive controls (ascorbic acid – AA or Trolox) at a concentration of 200 µM. Then, in order to initiate haemolysis 40 mM AAPH or 75 mM H<sub>2</sub>O<sub>2</sub> ice cold solutions in PBS (that were freshly prepared) were added to all the samples. The samples containing erythrocytes stressed by AAPH were incubated at 37°C up to 180 min, whereas these ones stressed by H<sub>2</sub>O<sub>2</sub> – up to 210 min. Finally, the absorbance of the supernatant obtained after centrifugation (1000 rpm, 5 min) of each sample was measured spectrophotometrically at  $\lambda_{\max}$  524 nm (in the case of haemolysis induced by AAPH) or  $\lambda_{\max}$  540 nm (in the case of haemolysis induced by H<sub>2</sub>O<sub>2</sub>). The antihaemolytic effects of positive controls – AA or Trolox – were defined as 1, whereas the antihaemolytic activities of compounds that were investigated were calculated in relation to AA or Trolox.

#### 2.1.6. Chromatographic measurements

For RP-HPLC measurements the Shimadzu Vp liquid chromatographic system (Shimadzu, Izabelin, Poland) (equipped with LC 10AT pump, SPD 10A UV-VIS detector, SCL 10A system controller, CTO-10 AS chromatographic oven and Rheodyne injector valve with a 20 µL loop) was employed. The test analytes were detected under ultraviolet light at  $\lambda_{\max}$  254 nm. All the chromatographic measurements were carried out in isocratic conditions at 25°C (298 K). The dead time values were measured from citric acid (Avantor Performance Materials, Poland) peaks. For calculation of the retention factors average values from at least three independent experimental measurements were taken. The retention factor,  $k$ , was calculated as follows:

$$k = \frac{(t_R - t_0)}{t_0}$$

where  $t_R$  denotes the retention time of an analysed sample and  $t_0$  is the retention time of citric acid as an unretained marker.

The endcapped octadecyl silica column (ODS) and the column with immobilised artificial membrane (IAM) were employed as two stationary phases of choice for RP-HPLC measurements.

As mobile phases buffer-acetonitrile mixtures were used. The buffer was prepared from 0.01 M L<sup>-1</sup> solutions of Na<sub>2</sub>HPO<sub>4</sub> (Avantor Performance Materials, Poland) and citric acid, and the pH 7.4 value was fixed before mixing with acetonitrile (HPLC grade) as an organic modifier. Acetonitrile concentration in the effluent, expressed as a volume fraction, was changed in the range 0.3-0.6 (ODS column) or 0.3-0.5 (IAM column), at a flow rate of 1.0 mL min<sup>-1</sup> with the ODS column and 1.2 mL min<sup>-1</sup> with the IAM column. A double distilled water was obtained from a Direct-Q 3 UV apparatus (Millipore, Poland).

#### 2.1.7. *In silico* calculations

The following pharmacokinetic descriptors: Caco-2, log  $K_{a, HSA}$  and  $f_{u, brain}$ , log  $K_p$  were calculated from molecular structures of the investigated compounds according to the model of Abraham based on linear solvation energy relationships (LSERs) [23] using the ACD/Percepta software (Łódź, Poland).

The *n*-octanol/water partition coefficients were provided as average values (log  $P_{average}$ ) taken from all accessible computational algorithms (*e.g.* Alog P<sub>s</sub>, AC log P, milog P, Alog P, Mlog P, Xlog P2 and Xlog P3). All the computational log  $P$  values were obtained from molecular structures of the examined compounds using an online software (<http://www.vcclab.org/>).

#### 2.1.8. Statistical calculations

All biological experiments were carried out at least in triplicate. The obtained results were averaged and the data are given as the mean ± SD. Statistical analyses were done by the use of a STATISTICA 12.5PL programme (StatSoft, Kraków, Poland). The p values less than 0.05 were considered as statistically significant.

Statistical analyses in a chromatographic part of the paper were performed employing the Minitab 16 software (Minitab Inc., State College, Pennsylvania, USA).

### 3. Results and discussion

#### 3.1. Synthesis of two novel classes of bicyclic nucleobase-like compounds (9-16 and 17-22)

The total synthesis of the starting functionalised nucleophiles (**1-8**, *e.g.* 1-substituted-2-hydrazinylideneimidazolidine hydroiodides) (Scheme 1) was achieved in two individual steps. At first, 1-substituted-4,5-dihydro-1*H*-imidazole-2-thiols were alkylated using

equimolar ratios of methyl iodide in methanolic medium to yield 2-methylsulfanyl-1-substituted-4,5-dihydro-1*H*-imidazole hydroiodides. Next, they were subjected to condensation with hydrazine hydrate in methanolic medium under reflux giving rise to the desired 2-hydrazinylidene-1-substituted-imidazolidine hydroiodides, as previously described [6,21,22].

We have previously examined extensively different reactions of imidazolidine hydrazones (as building block units) with a variety of two-carbon atom donors. In general, we have found that numerous fused azaisocytosine-like congeners as the final products formed in these reactions reveal interesting anticancer activities [4-6,8,11,18,20,21]. Therefore, we decided to extend our studies to other unknown fused azaisocytosine-containing congeners as new possible bioisosteres with potential utility in medicine. To the best of our knowledge, this is the first research report that describes the reactions of 1-substituted-2-hydrazinylideneimidazolidine hydroiodides (**1-8**) with ethyl trifluoropyruvate or ethyl 3-methyl-2-oxobutyrate leading to two novel classes of unknown small molecules (Scheme 1). Furthermore, 1-substituted-2-hydrazinylideneimidazolidines and their hydrohalide salts have not been hitherto treated with ethyl trifluoropyruvate or ethyl 3-methyl-2-oxobutyrate with the goal of obtaining the target (**9-22**) or other compounds. Hence, we have developed two novel approaches of choice that can be used in preparing two important classes of nucleobase-like molecules (**9-16** and **17-22**) [24-26]. Using these relatively simple and good-yielding synthetic routes (that utilise ethyl trifluoropyruvate or ethyl 3-methyl-2-oxobutyrate as excellent annelation electrophiles and functionalised imidazolidines as the starting precursor units, revealing a high nucleophilicity towards electrophilic reagents) we were able not only to construct the privileged 7,8-dihydroimidazo[2,1-*c*][1,2,4]triazin-4(6*H*)-one template but in addition to introduce to this drug-like scaffold two desired groups (*e.g.* the trifluoromethyl or isopropyl moiety – revealing a similar rotational barrier) at the *C*-3 and a variety of aromatic substituents at the *N*-8. The goal in this case was to identify some molecules belonging to both structurally diverse classes of novel fused azaisocytosine-containing congeners with the best substitution patterns for anticancer activities or selectivities.

The general synthetic procedure, which was developed to obtain the two original classes of fused azaisocytosine-containing congeners (**9-16** and **17-22**), is based on the successive heteroannelation strategy. This synthetic approach proved effective with **9** (R = C<sub>6</sub>H<sub>5</sub>), **10** (R = 2-CH<sub>3</sub>C<sub>6</sub>H<sub>4</sub>), **11** (R = 4-CH<sub>3</sub>C<sub>6</sub>H<sub>4</sub>), **12** (R = 2-OCH<sub>3</sub>C<sub>6</sub>H<sub>4</sub>), **13** (R = 2-ClC<sub>6</sub>H<sub>4</sub>), **14** (R = 3-ClC<sub>6</sub>H<sub>4</sub>), **15** (R = 4-ClC<sub>6</sub>H<sub>4</sub>), **16** (R = 3,4-Cl<sub>2</sub>C<sub>6</sub>H<sub>3</sub>) belonging to the trifluoromethyl class, and also with **17** (R = C<sub>6</sub>H<sub>5</sub>), **18** (R = 4-CH<sub>3</sub>C<sub>6</sub>H<sub>4</sub>), **19** (R = 2-ClC<sub>6</sub>H<sub>4</sub>), **20** (R = 3-ClC<sub>6</sub>H<sub>4</sub>), **21** (R =

4-ClC<sub>6</sub>H<sub>4</sub>), **22** (R = 3,4-Cl<sub>2</sub>C<sub>6</sub>H<sub>3</sub>) belonging to the isopropyl series. In this case the triazinone template was annelated on the pre-existing functionalised imidazolidines (**1-8** in the case of the trifluoromethyl series and **1, 3, 5-8** in the case of the isopropyl series). However, surprisingly the strategic approach – leading to construction of the “right-hand” triazinone template on 1-(2-methylphenyl)- / 1-(2-methoxyphenyl)-2-hydrazinylideneimidazolidine derivatives using ethyl 3-methyl-2-oxobutyrate as an annelation reagent – failed. Thus it was not possible to obtain these two final products belonging to the isopropyl class under any conditions studied.

Because of a high degree of conjugation of double bonds within the triazinone template (*e.g.* C=N, C=N and C=O), all the obtained molecules (**9-22**), proved to be stable in organic solvents. This well agrees with the Hückel’s rule for cyclic conjugated systems possessing aromatic stability.

The most likely mechanism for the formation of 8-substituted-3-(trifluoromethyl)-7,8-dihydroimidazo[2,1-*c*][1,2,4]triazin-4(6*H*)-ones (**9-16**) and 8-substituted-3-(propan-2-yl)-7,8-dihydroimidazo[2,1-*c*][1,2,4]triazin-4(6*H*)-ones (**17-22**) was formulated according to the Scheme 1. Both synthetic pathways leading to the unknown compounds (**9-16** and **17-22**) were hypothesised to proceed *via* the most probable intermediates (**A, B, C, D**). In the first step, the nitrogen-containing nucleophiles, differently substituted at the *N*-1, *e.g.* 1-(*R*-phenyl)-2-hydrazinylidenimidazolidine hydroiodide salts (**1-8**), underwent addition to the  $\alpha$ -carbonyl group of the suitable electrophiles, such as ethyl trifluoropyruvate or ethyl 3-methyl-2-oxobutyrate, under basic conditions. As a result of this step the initial formation of hemiaminal intermediates (*e.g.* ethyl 3,3,3-trifluoro-2-hydroxy-2-[(*2E*)-2-(1-substituted-imidazolidin-2-ylidene)hydrazinyl]propanoates (**A**) and ethyl 2-hydroxy-3-methyl-2-[(*2E*)-2-(1-substituted-imidazolidin-2-ylidene)hydrazinyl]butanoates (**B**), respectively) would seem possible. Both intermediates (**A** and **B**) *via* subsequent dehydration could be further transformed into the most probable imine intermediates (*e.g.* ethyl 3,3,3-trifluoro-2-[(1-substituted-imidazolidin-2-ylidene)hydrazinylidene]propanoates (**C**) and ethyl 3-methyl-2-[(1-substituted-imidazolidin-2-ylidene)hydrazinylidene]butanoates (**D**), respectively). This exothermic reaction step (occurring in both cases with a concomitant loss of one water molecule and formation of triethylammonium iodide – Et<sub>3</sub>NH<sup>+</sup>I<sup>-</sup> – as a by-product of alkylation) proved successful when the synthetic process was carried out in two-component polar protic and aprotic solvent media (such as *n*-butanol/DMF mixture) or in polar solvent (such as *n*-butanol) containing a small molar excess of triethylamine. In the second step of the proposed mechanism, both series of imine intermediates (**C** and **D**) were transformed into two novel classes of the highly conjugated fused azaisocytosine-containing congeners (**9-16** and

**17-22**) *via* intramolecular heterocyclisation accomplished by a closure of the triazinone scaffold. This final step (occurring with a concomitant elimination of one ethanol molecule) was performed successfully under established reaction conditions (*e.g.* on heating under reflux in the suitable two-component polar solvent mixtures such as MeOH/DMF or on refluxing in an appropriate polar solvent such as *n*-BuOH). The course of heterocyclisation leading to the title compounds **9-22** was confirmed experimentally. It was proven that it proceeds in the direction which yields the most stable products possessing the least energy. Thus, as expected, it is thermodynamically preferred. It was also confirmed that a small molar excess of triethylamine during heterocyclisation results in much higher yields of the synthesised fused azaisocytosine-containing congeners.

The occurrence of the suggested mechanism was confirmed by isolating the stable nucleobase-like products belonging to both novel classes (**9-16** and **17-22**) and based on a thorough exploration of the reaction mother liquors. This examination proved that under well-established reaction conditions the hydrogen iodide (from 1-substituted-2-hydrazinylidenemidazolidines) had reacted with triethylamine to yield Et<sub>3</sub>NH<sup>+</sup>I<sup>-</sup> as a by-product of alkylation. Besides, it should be noted that when the crude products (**9-22**) were precipitated, filtered off, washed with water, cold methanol and finally were subjected to recrystallisation from suitable organic solvents mixtures or a solvent, they proved to be the sufficiently lower soluble than a by-product of alkylation. Hence, Et<sub>3</sub>NH<sup>+</sup>I<sup>-</sup> could be successfully removed and the final fused azaisocytosine-containing products (**9-22**) could be isolated in a pure state.

### 3.2. Spectroscopic characterisation of two novel classes of compounds (**9-16** and **17-22**)

The structural determination of 8-substituted-3-(trifluoromethyl)-7,8-dihydroimidazo[2,1-*c*][1,2,4]triazin-4(6*H*)-ones (**9-16**) and 8-substituted-3-(propan-2-yl)-7,8-dihydroimidazo[2,1-*c*][1,2,4]triazin-4(6*H*)-ones (**17-22**) was performed using spectroscopic experiments. The <sup>1</sup>H NMR, ATR-IR and UV-VIS spectra were consistent with the assigned structures of all the compounds that were synthesised as well as with electronic transitions in their molecules.

The <sup>1</sup>H NMR spectra of **9-16** and **17-22** in DMSO-*d*<sub>6</sub> and CDCl<sub>3</sub>, respectively, although displaying some spectral similarities (such as a multiplet signal – in the region around 4.02-4.35 ppm and integrating for four protons – which can be assigned to both endocyclic methylene groups belonging to the imidazolidine ring), revealed in addition the

significant spectral difference because of a different substitution pattern at the C-3 in both classes of molecules. Barely, in case of compounds **17-22** a typical doublet (at  $\delta$  in the region around 1.27-1.31 ppm with a coupling constant of  $J = 6.9$  Hz and integrating for six protons) confirmed the presence of both methyl groups ( $\text{CH}(\text{CH}_3)_2$ ) belonging to the isopropyl moiety, while multiplet signals at  $\delta$  in the region around 3.28-3.33 ppm (and integrating for one proton) affirmed the attendance of the methine group ( $\text{CH}(\text{CH}_3)_2$ ) belonging to the same moiety. In turn, compounds **9-16** were devoid of any proton signals in above-mentioned regions, as expected, since they have not any hydrogen atoms at the C-3.

The ATR-IR spectra of **9-22** in the solid state, although showing some spectral similarities (such as strong absorption bands in the ranges 1674-1709 and 1550-1565 that can be assigned to the stretching vibrations of C=O group and the C=N bond at the ring junction (*i.e.* C8a=N1), respectively) due to the presence of the common completely conjugated 1,2,4-triazinone system in both compound series, displayed additionally the main spectral difference resulting from various substitution patterns at the C-3 in both classes of compounds. Characteristic absorption bands were registered in the ATR-IR spectra of **9-16** due to the presence of the trifluoromethyl group, displaying numerous vibrational frequencies in the range 1333-1126  $\text{cm}^{-1}$ . In turn, diagnostic absorption bands were seen in the ATR-IR spectra of **17-22** owing to the presence of the isopropyl group. There was a visible splitting of the symmetric  $\text{CH}_3$  scissor vibrations into two bands (of similar intensity) that are positioned at *ca.* 1381 and 1370  $\text{cm}^{-1}$ .

Ultraviolet spectroscopic investigations of the diluted methanolic solutions of **9-22** revealed two characteristic absorption bands that can be assigned to two electronic transitions within the molecules under study (*i.e.*  $\pi \rightarrow \pi^*$  and  $n \rightarrow \pi^*$ ). The most likely is that the completely conjugated fused azaisocytosine (*e.g.* 1,2,4-triazin-5(4*H*)-one) template (containing the conjugated system of chromophores: C=N, C=N with a lone pair of electrons at the  $\text{sp}^2$  hybridised nitrogen atom and C=O), which is present in both classes of the studied compounds (**9-16** and **17-22**), is capable of absorbing an ultraviolet light at the band maximum of lower intensity in the wavelength ranges 302.0-329.5 nm because of the most characteristic  $n \rightarrow \pi^*$  (*R*) electronic transition. The presence of the second UV band maximum of higher intensity in the wavelength region around 230.0-266.5 nm in case of all the compounds (**9-22**) can be rationally explained by the possible  $\pi \rightarrow \pi^*$  (*K*) electronic transition within their molecules. It has been confirmed experimentally, as expected, that extinction coefficients for absorption bands characteristic to  $\pi \rightarrow \pi^*$  electronic transitions are

higher, whereas extinction coefficients for absorption bands characteristic to  $n \rightarrow \pi^*$  electronic transitions are lower.

### 3.3. Antiproliferative effects of novel fused azaisocytosine-containing congeners (**9-16** and **17-22**)

The majority of test compounds at a concentration of 0.176 mM were effective at inhibiting the proliferation in three tumour cell cultures recruited (A549, T47D and HeLa) (Table 1; Fig. S2 in Supplementary material). Compounds bearing the isopropyl moiety (**17-22**) proved to be more active against HeLa cells (especially after 24 h of incubation) than trifluoromethylated structures (**9-16**). In turn, most molecules containing the trifluoromethyl moiety (except *ortho*- and *para*-chloro substituted derivatives, *i.e.* **13** and **15**) were more cytotoxic against A549 cells (after 48-72 h). However, both classes of molecules revealed comparable antiproliferative effects in T47D cells.

It should be noted that the majority of test molecules evoked higher antiproliferative effects in tumour cells than pemetrexed at the same concentration (0.176 mM). Simultaneously, all 8-(*R*-phenyl)-3-trifluoromethyl-7,8-dihydroimidazo[2,1-*c*][1,2,4]triazin-4(6*H*)-ones bearing the *ortho* substitution at the phenyl ring (**10**, **12** and **13**) proved to be less or equally toxic to normal Vero cells (after all incubation periods) as pemetrexed at the same concentration. According to current concepts the capacity of test innovative nucleobase-like compounds to inhibit proliferation of tumour cells is most likely the result of their competition for nucleobases required for DNA synthesis [4,5].

Amongst 8-(*R*-phenyl)-3-trifluoromethyl-7,8-dihydroimidazo[2,1-*c*][1,2,4]triazin-4(6*H*)-ones the parent compound (**9**), without substitution at the electron-rich phenyl moiety, showed the highest percentage of growth inhibition in T47D cells (after 24 h of incubation).

Introducing an electron-donating methyl group *ortho* to the phenyl moiety (the structure **10**) caused only slight changes in antiproliferative potencies in A549 cell line, when compared to **9**. However, placing an electron-donating methyl group *para* to the phenyl ring (the molecule **11**) enhanced cytotoxicities against A549 cells (after all incubation periods), but diminished antiproliferative effects against T47D cells after 24 h of incubation. It should be noted that the *ortho*- and *para*-methyl substitution patterns are favourable due to reduction in cytotoxicities against non-tumoural Vero cells (after 24-72 h), when compared to the parent counterpart (**9**). Notwithstanding, the *ortho*-methyl substitution pattern in **10** was more profitable than a *para*-methyl one in **11** in terms of the increased selectivity.

Replacing the methyl group *ortho* to the phenyl moiety by an electron-donating methoxy substituent (**12**) at the same position enhanced antiproliferative potencies against A549 cells (after 24-72 h of incubation). Both substitution patterns (*ortho*-methyl and *ortho*-methoxy) resulted in more selective molecules (**10** and **12**), when compared to **9**, showing decreased toxicities to Vero cells (after all incubation periods).

Replacing the methyl group at the *para* position in **11** with an electron-withdrawing chloro substituent located at the same position in **15** was unsuccessful due to a decrease in antiproliferative effects especially in A549 cell line (after all incubation periods) and an increase in cytotoxicities towards normal Vero cells (after 24 h of incubation).

Moving the chloro substituent from the *para* to the *ortho* or *meta* position of the phenyl moiety produced the evidently potent structures (**13** or **14**) against A549 cells (after 24-72 h of incubation), in comparison to **15**. Additionally, the *ortho*-chloro substituted derivative (**13**) was identified as a very low toxic molecule towards normal Vero cells (after all incubation periods).

Introducing a further chloro group to the *meta*-chloro (**14**) or *para*-chloro (**15**) derivative enhanced antiproliferative effects of 3,4-dichloro-substituted counterpart (**16**) in tumour cells recruited (especially in A549 cells after all incubation periods when compared to **15** and in HeLa cells after 48-72 h when compared to **14**).

The majority of 8-(*R*-phenyl)-3-(propan-2-yl)-7,8-dihydroimidazo[2,1-*c*][1,2,4]triazin-4(6*H*)-ones evoked remarkable antiproliferative effects in T47D and HeLa cells, while displaying less cytotoxic effects towards A549 cells.

Putting a methyl group *para* to the phenyl ring (structure **18**) evoked an increase in cytotoxicity against T47D cells (after 24 h of incubation), when compared to the parent compound (**17**). In turn, this modification resulted in an increase of the cytotoxicity against Vero cells (after all incubation periods), comparatively to **17**.

The replacement of the methyl group at the *para* position of the phenyl moiety (structure **18**) with a chloro substituent located at the same position allowed us to obtain the bioisostere **21**, revealing an enhanced cytotoxicity against A549 cells (especially after 72 h of incubation), while diminished antiproliferative effects against T47D and HeLa cells (particularly after 24 h). Nevertheless, this modification was responsible for the significant reduction of cytotoxicity in normal cells (after all incubation periods).

Moving the chloro substituent from the *para* to the *ortho* position of the phenyl ring was tolerated since resulted in the antiproliferative active structure (**19**), showing increased cytotoxicities in HeLa (after 24-72 h of incubation) and A549 (after 24 h) cells, when

compared to the compound **21**. Simultaneously, this modification did not alter cytotoxicities towards Vero cells (after all incubation periods). In turn, moving the chloro substituent from the *para* to the *meta* position of the phenyl moiety was favourable. This modification led to the structure **20** revealing increased antiproliferative effects in HeLa (after 48-72 h of incubation) and A549 (after 24 h) cells, comparatively to the compound **21**.

Introducing an additional chloro group to the *meta*-chloro (**20**) or *para*-chloro (**21**) derivative enhanced cytotoxicities of the 3,4-dichloro-substituted counterpart (**22**) against T47D and A549 cells (after 48 h of incubation).

Concluding, the methyl, methoxy and chloro groups in the *ortho* position (in the case of 8-(R-phenyl)-3-trifluoromethyl-7,8-dihydroimidazo[2,1-*c*][1,2,4]triazin-4(6*H*)-ones) as well as the chlorine atom in the *ortho* and *para* positions (in the case of 8-(R-phenyl)-3-(propan-2-yl)-7,8-dihydroimidazo[2,1-*c*][1,2,4]triazin-4(6*H*)-ones) of the phenyl moiety were found to be the best choices of substitution patterns in terms of the increased selectivity. Thus, an attention should be focused on five antiproliferative active structures (**10**, **12**, **13**, **19** and **21**), revealing the lowest cytotoxicities towards non-tumoural cells. Hence, these ones will be utilised in design of less toxic anticancer agents.

Comparing the antiproliferative activities against tumour cells and cytotoxicities to normal cells of previously synthesised antitumour active fused azaisocytosine-containing congeners with ethyl substitution at the C-3 [5] and their bioisosteres with the trifluoromethyl (**9-16**) or isopropyl (**17-22**) groups (presenting a comparable steric arrangement) it was found that modifications resulting from isosterism are profitable in terms of selectivity in both classes of novel compounds. It should be noted that the rationally modified bioisosteres proved to be less toxic to normal cells (except **18**) (Table 2), retaining the same type of biological activity, *i.e.* the anticancer profile.

#### 3.4. The $IC_{50}$ values and selectivity indices of novel fused azaisocytosine-containing congeners (**9-22**)

The  $IC_{50}$  values of all test compounds (**9-22**) are listed in Table 3. The selectivity indices (SIs – the  $IC_{50}$  values of test compounds in a non-tumoural cell line divided by the  $IC_{50}$  values of test compounds in a tumour cell line) of **9-22** are presented in Table 4.

Analysing all selectivity indices, the majority of test compounds proved to be the most selective for T47D cell line, revealing SIs better or comparable to that of 4-hydroxytamoxifen, which is clinically approved for the treatment of human breast cancer (SI = 1.29) [27]. High

SI ratios were also observed for most test compounds in the HeLa cell line and for some in the A549 cell line. It can be assumed that promising compounds possessing better selectivity indices should cause less damage to the epithelium of the gastrointestinal tract. This promising finding justifies their further *in vivo* testing.

Moreover, replacing the ethyl group (which is sensitive to oxidation) by a trifluoromethyl group at the C-3 of fused azaisocytosine nucleus would increase the metabolic stability of bioisosteres **9-16** against biotransformation since the CF<sub>3</sub> group possessing the strength C–F bond is biostable.

The majority of novel compounds revealed better selectivity indices than that of pemetrexed in A549 (**11, 12, 13, 14, 16**), T47D (**9, 10, 11, 12, 13, 14, 15, 16, 17, 19, 20, 21, 22**) and HeLa (**10, 11, 12, 13, 15, 16, 17, 19, 20, 21**) cell lines. Simultaneously, most of molecules with the trifluoromethyl moiety demonstrated better selectivity indices (after 48- and 72-h incubation periods) than their counterparts with the isopropyl group. Some of compounds were about twice less cytotoxic to non-tumoural than cancer cells, which indicates a large safety window.

### 3.5. The effect of the compound **12** on caspase-6 and -8 levels in normal and cancer cells

Caspases – cysteine-dependent aspartate-directed proteases – play a key role in the initiation and execution of apoptosis as programmed cell death. From a therapeutic point of view, compounds capable of inducing apoptosis are particularly important to evoke apoptosis in cancer cells. Therefore, the search for new synthetic activators of caspases is still attractive in the field of anticancer drug discovery [28-31].

Among the most promising fused azaisocytosine-containing congeners, the compound **12** – with an enhanced antitumour activity and simultaneously safe for normal cells (Tables 1 and 4) – was chosen to evaluate its effect on caspase-6 and -8 levels in normal and cancer epithelial cells (Table 5). The molecule **12** was shown to have no effect on caspase-6 and -8 levels – compared to control – in normal Vero cells. This may be due to its very low toxicity towards these non-tumoural cells. In turn, the test compound was able to induce the caspase-mediated apoptosis in some cancer cells. This was confirmed by a significant increase in the level of caspase-6 (*e.g.* an executioner of apoptosis) in tumour cells of lung and breast as well as the level of caspase-8 (*e.g.* an initiator of apoptosis) in tumour cells of lung. Therefore, it can be deduced from the above-mentioned results that the antiproliferative activity of **12** may be associated with the activation of caspases which are inducers of apoptosis.

### 3.6. Antihaemolytic effects of novel fused azaisocytosine-containing congeners (9-22)

The antihaemolytic activities of fused azaisocytosine-containing congeners (9-22) at a concentration close to the  $IC_{50}$  values (*i.e.* 200  $\mu$ M) were assessed on *ex vivo* model of rat erythrocytes. In this study, the oxidative haemolysis of red blood cells is induced by 2,2'-azobis(2-methylpropionamide) dihydrochloride (AAPH; peroxy radical generator) or hydrogen peroxide ( $H_2O_2$ ). The preincubation of erythrocytes with test compounds can exert protective effect against oxidative damage of red blood cell membranes.

Almost all fused azaisocytosine-containing congeners proved to be very effective at inhibiting the oxidative haemolysis of erythrocytes exposed to AAPH as well as  $H_2O_2$  (Figs 1A and B). It is noteworthy that the antihaemolytic activities of all 8-substituted-3-trifluoromethyl-7,8-dihydroimidazo[2,1-*c*][1,2,4]triazin-4(6*H*)-ones (9-16) were better than that of standard drugs – ascorbic acid (AA) (when AAPH was used to initiate haemolysis) and Trolox (when  $H_2O_2$  was used to generate haemolysis). In turn, the majority of 8-substituted-3-(propan-2-yl)-7,8-dihydroimidazo[2,1-*c*][1,2,4]triazin-4(6*H*)-ones revealed more protective effects than AA on erythrocytes exposed to AAPH. Additionally, most of them showed better or comparable antihaemolytic activities than Trolox when erythrocytes were treated with  $H_2O_2$ .

Taking into account the obtained results, these promising compounds – due to their protective effects on oxidatively stressed erythrocytes – should not induce haemolytic anaemia in the organism. Therefore, these novel biologically active molecules may be considered as non-toxic, without side effects on red blood cells.

### 3.7. Lipophilicity indices of test compounds

Reversed-phase chromatographic measurements were carried out employing aqueous buffered systems, which contain different volume fractions of acetonitrile as an organic modifier, as mentioned in the experimental section. In the present study the standardised lipophilicity indices,  $\log k_w$  of all the solutes (9-22) were used.  $\log k_w$  were calculated by the linear extrapolation to 0% of acetonitrile in the mobile phase from relationships that were established for retention on the endcapped octadecylsilica column (ODS) and column with immobilised artificial membrane (IAM) between the logarithmic retention factors ( $\log k$ ) and

the concentration of acetonitrile in the eluent, using the semilogarithmic linear equation of Soczewiński-Wachtmeister [32].

Highly statistically significant rectilinear correlations (with square correlation coefficients very close to 1), which were obtained between two chromatographic parameters from the equation of Soczewiński-Wachtmeister such as intercepts ( $\log k_w$ ) and slopes ( $s$ ), on both RP-HPLC columns (such as ODS and IAM) confirmed the congenerity of test series of molecules:

$$\log k_{w,ODS} = -0.967219 (\pm 0.0870281) + 0.89819 (\pm 0.0251385) s_{ODS} \quad (\text{Eq. 1})$$

$$S = 0.0441336, R^2 = 0.9907, F = 1276.61, p = 0.0000000$$

$$\log k_{w,IAM} = -0.193068 (\pm 0.0397860) + 0.550403 (\pm 0.0147489) s_{IAM} \quad (\text{Eq. 2})$$

$$S = 0.0465726, R^2 = 0.9915, F = 1392.64, p = 0.0000000$$

Both relationships (Eq. 1 and 2) were additionally shown graphically in Figs 2A and B, respectively. Taking into account the linearity of these relationships it was proven that  $\log k_w$  and  $s$  values are reliable alternative lipophilicity descriptors satisfying the theory and definition of the  $\log k_w$  [23,33] and characterising the lipophilicity scale and chromatographic behaviour on two different reversed-phases of novel congeneric small molecules that were investigated.

The statistically significant and very good linear correlation (presented graphically in Fig. 3) was obtained between the  $\log k_{w,IAM}$  and  $\log k_{w,ODS}$  values:

$$\log k_{w,IAM} = -1.05661 (\pm 0.147958) + 1.07579 (\pm 0.068640) \log k_{w,ODS} \quad (\text{Eq. 3})$$

$$S = 0.108745, R^2 = 0.9534, F = 245.639, p = 0.0000000$$

The parameters of Eq. 3 and statistical terms are listed in Table S1 in Supplementary material.

The analysed congeners belonging to the first class (**9-16**) proved to be more lipophilic than congeneric molecules belonging to the second series (**17-22**) (Table S1 in Supplementary

material). This may be caused by the presence of the trifluoromethyl substituent which is larger in size than the isopropyl group and mimics the more lipophilic isobutyl moiety [34].

Lipophilicity profiles of molecules **9-22**, which were determined experimentally ( $\log k_{w, \text{IAM}}$ ,  $\log k_{w, \text{ODS}}$ ) and computed ( $\log P_{\text{average}}$ ), are presented in Fig. 4. Novel experimental lipophilicity profiles showed that there exist a strict compliance in the retention trend for all analysed molecules on both reversed stationary phases.

Generally, the  $\log k_w$  indices of the *ortho*-substituted compounds (**10**, **13** and **19**) were found to be lower than those of the *para*- and *meta*-substituted molecules (**11**, **15**, **21** and **14**, **20**, respectively) (Table S1 in Supplementary material). It was confirmed that substituents in the *ortho* position at the phenyl ring decrease the  $\log k_w$  values of test molecules in the following order:  $\text{Cl} > \text{CH}_3 > \text{CH}_3\text{O}$ . This *ortho* effect is clearly seen in the case of bioisosteres **10**, **12** and **13** bearing the trifluoromethyl group at the *C*-3. It is well known that the substituents in the *ortho* position are capable of hindering the free rotation of the phenyl ring, which results in decreased lipophilicity parameters (the so-called *ortho* effect) [35-37].

It was found generally that the *para* and *meta* substitution at the phenyl moiety increases the  $\log k_w$  indices, whereas the *ortho* substitution decreases these ones, in relation to the parent compounds (*e.g.* **9** and **17**). Molecules bearing *meta*-chloro substitution at the phenyl ring (**14** and **20**) proved to be slightly more lipophilic than those containing *para*-chloro substitution (**15** and **21**). In turn, it was proven that placing the second chlorine atom to the *para*- or *meta*-chloro derivatives increases the  $\log k_w$  values of both 3,4-dichloro-substituted solutes (**16** and **22**) (Table S1 in Supplementary material).

The relationships between *n*-octanol/water logarithmic partition coefficients expressed as  $\log P_{\text{average}}$  values (that were calculated from molecular structures of test compounds using an online programme <http://www.vcclab.org/>) and experimentally determined standardised  $\log k_w$  indices were thoroughly studied, using a linear regression. It was found that  $\log P_{\text{average}}$  versus  $\log k_w$  dependences are linear for eleven test compounds (**9**, **11-12**, **14-18**, **20-22**) (Figs 5A and B). The statistically significant and very good linear correlation was obtained between  $\log P_{\text{average}}$  coefficients and extrapolated  $\log k_{w, \text{ODS}}$  indices of eleven solutes (Fig. 5A). In addition, the statistically significant and good linear relationship was found between  $\log P_{\text{average}}$  values and extrapolated  $\log k_{w, \text{IAM}}$  indices of eleven analytes (Fig. 5B). The statistical terms for both equations are presented underneath Figs 5A and B. In turn, there were severe objections against calculated lipophilicities for three *ortho*-substituted outliers (**10**, **13** and **19**), meaning that the prediction of reliable  $\log P_{\text{average}}$  coefficients for these

molecules is impossible and therefore the computed results have to be verified experimentally.

### 3.8. Principal component analysis

The overall data set variables were submitted to the PCA-based approach as a tool for multivariate data projection in order to obtain linear combinations (the so-called principal components – PCs) visualising the relationships between the standardised  $\log k_{w, \text{IAM}}$ ,  $\log k_{w, \text{ODS}}$  values, computed *n*-octanol/water logarithmic partition coefficients (expressed as  $\log P_{\text{average}}$ ) and *in silico* pharmacokinetic descriptors of the studied compounds such as: Caco-2 permeability values (meaning the permeability coefficients through the intestinal epithelium of Caco-2 cells),  $\log K_{a, \text{HSA}}$  values (showing affinity constants to human serum albumin),  $f_{u, \text{brain}}$  (meaning the fraction unbound (*e.g.* active) in brain tissue) and  $\log K_p$  values (describing skin permeation coefficients). When plots of the first 3 principal components were considered it was found that they explained 96.9% of the total variance of the data. It should be noted that the first 2 principal components (*PC1* vs *PC2*) explained more than 92% of the total variance. The relationships between these data matrices are presented graphically in Fig. 6A. There is seen on the *PC1* vs *PC2* plot that three *in silico* pharmacokinetic descriptors (*e.g.* Caco-2,  $\log K_p$  and  $\log K_{a, \text{HSA}}$ ) are directly proportional to the computed  $\log P_{\text{average}}$  coefficients and the standardised lipophilicity indices that were determined experimentally ( $\log k_{w, \text{ODS}}$  and  $\log k_{w, \text{IAM}}$ ). This indicates that there is a high correlation between these variables, revealing positive values of the first principal component. In turn, there is visible on the same *PC1* vs *PC2* plot that  $f_{u, \text{brain}}$  predictor is inversely proportional to the empirical logarithms of retention factors ( $\log k_{w, \text{ODS}}$  and  $\log k_{w, \text{IAM}}$ ) and to the predicted  $\log P_{\text{average}}$  values since its first principal component reveals a negative value. Similarities and dissimilarities between properties of the analysed molecules in relation to chromatographic, partitioning and pharmacokinetic variables are shown in Fig. 6B. Since test two classes of congeners (**9-16** and **17-22**) contained the trifluoromethyl or isopropyl group, respectively, attached to the *C*-3 of the scaffold (presenting a comparable steric arrangement) their clustering (Fig. 6B) indicates that the most significant structural factor influencing their properties is the substitution at the *N*-8 of the template. Thus, they are divided into three distinctive clusters. The first cluster is formed by two molecules of both classes which are substituted at the *N*-8 by the phenyl ring (**9**, **17**) and one which is substituted by the methoxyphenyl moiety (**12**). The largest second cluster is created by compounds having at the *N*-8 the mono-methylphenyl or mono-

chlorophenyl substitution (**10**, **11**, **13-15**, **18-21**), whereas the third cluster is formed by molecules possessing the 3,4-dichlorophenyl substitution (**16**, **22**).

### 3.9. Correlations between lipophilicity parameters and *in silico* pharmacokinetic descriptors

The  $\log K_{a,HSA}$  values of test compounds' (meaning the affinity constants to human serum albumin (HSA) as the most abundant protein of plasma [14,38], which are listed in Table S2 in Supplementary material) were correlated with experimentally assessed lipophilicity indices on both stationary phases ( $\log k_{w, ODS}$  and  $\log k_{w, IAM}$ ) and computed  $\log P_{average}$  coefficients. The following statistically significant QSAR equations were derived for describing the  $\log K_{a,HSA}$  of eleven molecules tested (**9**, **11**, **14-18**, **20-22**) in terms of their experimentally determined lipophilicity indices and computed partition coefficients:

$$\log K_{a,HSA} = 3.73957 (\pm 0.331976) - 0.0719538 (\pm 0.256002) \log P_{average} + 0.721998 (\pm 0.255965) \log k_{w,ODS} \quad (\text{Eq. 4})$$

$$\text{where } S = 0.0973882, R^2 = 0.8979, F = 30.7855, p = 0.000340$$

$$\log K_{a,HSA} = 4.10530 (\pm 0.369173) + 0.110069 (\pm 0.169252) \log P_{average} + 0.496327 (\pm 0.149865) \log k_{w,IAM} \quad (\text{Eq. 5})$$

$$\text{where } S = 0.0888518, R^2 = 0.9150, F = 37.6899, p = 0.000179$$

This indicates that the extrapolated lipophilicity indices,  $\log k_{w, ODS}$  and  $\log k_{w, IAM}$  (derived with the linear model for acetonitrile-buffer systems on ODS and IAM columns) and computed  $\log P_{average}$  coefficients can be successfully applied to assess the binding affinity of test molecules to human serum albumin.

The significant linear correlations were shown between the  $\log K_{a,HSA}$  predictors (affecting the whole ADME-Tox profiling of anticancer active compounds) and their standardised retention parameters ( $\log k_{w, ODS}$  and  $\log k_{w, IAM}$ ) after removing three *ortho*-substituted molecules (**10**, **13** and **19**) as evident outliers. They predicted to have a greater affinity to human serum albumin (as the most abundant plasma protein) due to decreased retention factors resulting from the most likely steric effects hindering a rotational freedom of the aromatic phenyl moiety. As is seen in Figs S3A and B in Supplementary material, with increasing lipophilicity indices the distribution of test molecules in human serum albumin also increases. This observation is consistent with previous investigations carried out on immobilised artificial membrane-type columns imitating biosystems, which revealed linear

relationships between affinities of medicines or bioactive molecules to human serum albumin and determined experimentally retention parameters [23,39-42].

The relationships between the fraction unbound in brain ( $f_{u, \text{brain}}$ ), determined empirically  $\log k_w$  indices ( $\log k_{w, \text{ODS}}$  and  $\log k_{w, \text{IAM}}$ ) and computed  $\log P_{\text{average}}$  coefficients were also thoroughly studied. The *in silico* predicted  $f_{u, \text{brain}}$  values of test compounds are provided in Table S2 in Supplementary material. The following statistically significant QSAR equations were derived to describe the fraction unbound in brain tissue for a set of eleven solutes (**9**, **11-12**, **14-18**, **20-22**) in terms of their lipophilicity parameters (determined experimentally as well as computed):

$$f_{u, \text{brain}} = 0.872090 (\pm 0.171618) - 0.00465855 (\pm 0.138038) \log P_{\text{average}} - 0.240244 (\pm 0.136567) \log k_{w, \text{ODS}} \quad (\text{Eq. 6})$$

$$\text{with } S = 0.0523901, R^2 = 0.8415, F = 18.5860, p = 0.001584$$

$$f_{u, \text{brain}} = 0.812159 (\pm 0.227250) - 0.0993425 (\pm 0.105481) \log P_{\text{average}} - 0.130709 (\pm 0.091662) \log k_{w, \text{IAM}} \quad (\text{Eq. 7})$$

$$\text{with } S = 0.0553820, R^2 = 0.8229, F = 16.2642, p = 0.002337$$

Therefore, the extrapolated retention parameters, derived with the linear model for acetonitrile-buffer systems on ODS and IAM columns, as important chromatographic lipophilicity indices ( $\log k_{w, \text{ODS}}$  and  $\log k_{w, \text{IAM}}$ ) and computed average logarithmic partition coefficients ( $\log P_{\text{average}}$ ) can be applied to assess the free fraction of eleven biologically active molecules in brain.

The remarkable correlations were obtained between  $f_{u, \text{brain}}$  predictors and experimental lipophilicity parameters ( $\log k_{w, \text{ODS}}$  and  $\log k_{w, \text{IAM}}$ ), after removing three *ortho*-substituted molecules (**10**, **13** and **19**) as evident outliers (see Figs S4A and B in Supplementary material). The curvilinear shape of these correlations suggests that with increasing standardised retention parameters of test molecules the concentration of their fraction unbound in brain tissue decreases.

All the investigated anticancer active compounds proved to be highly permeable in Caco-2 cells (Table S2 in Supplementary material) taking into consideration the provided classification of permeability [43,44]. Hence, they should be easily transported passively through human jejunum. The *in silico* Caco-2 permeability values ranged from  $187 \times 10^{-6} \text{ cm sec}^{-1}$  for compound **17** to  $235 \times 10^{-6} \text{ cm sec}^{-1}$  for the most lipophilic molecule **16**.

The significant correlations were obtained between the Caco-2 permeability and  $\log k_{w, ODS}$  and  $\log k_{w, IAM}$  indices (derived with the linear model for acetonitrile-buffer systems on ODS and IAM columns) (Figs S5A and B in Supplementary material) after removing three *ortho*-substituted outliers (**10**, **13**, **19**). The curvilinear shape of these relationships suggests that there exist an optimal lipophilicity value with regards to the optimal intestinal absorption. The possible reasonable explanation might be that molecules not lipophilic enough are poorly permeable through a lipid bilayer of biomembranes.

In turn, the following statistically significant QSAR equations were derived for describing the Caco-2 permeability of a set of eleven solutes (**9**, **11-12**, **14-18**, **20-22**) in terms of their experimental lipophilicity indices and computational partition coefficients:

$$Caco2 = 129.294 (\pm 23.0187) + 9.37276 (\pm 18.5147) \log P_{average} + 24.3626 (\pm 18.3175) \log k_{w, ODS} \quad (\text{Eq. 8})$$

where  $S = 7.02697$ ,  $R^2 = 0.8457$ ,  $F = 19.1830$ ,  $p = 0.001443$

$$Caco2 = 132.964 (\pm 30.2352) + 20.2499 (\pm 14.0341) \log P_{average} + 12.0418 (\pm 12.1955) \log k_{w, IAM} \quad (\text{Eq. 9})$$

where  $S = 7.36848$ ,  $R^2 = 0.8303$ ,  $F = 17.1291$ ,  $p = 0.002012$

This indicates that the extrapolated retention indices,  $\log k_{w, ODS}$  and  $\log k_{w, IAM}$  (derived with the linear model for acetonitrile-buffer systems on ODS and IAM columns) and computed  $\log P_{average}$  coefficients can be employed to predict the jejunum permeability of eleven anticancer active test molecules.

In addition, the relationships between the ability of test compounds to penetrate the skin (expressed as their  $\log K_p$  coefficients listed in Table S2 in Supplementary material), their empirical standardised lipophilicity indices ( $\log k_{w, ODS}$  and  $\log k_{w, IAM}$ ) as well as computational  $\log P_{average}$  coefficients were carefully studied.

The following statistically significant QSAR equations could be derived to describe the permeability through the skin for all the test molecules (**9-22**) in terms of their chromatographical lipophilicity indices and computational partition coefficients:

$$\log K_p = -7.57949 (\pm 0.282574) + 0.501106 (\pm 0.129639) \log P_{average} + 0.115728 (\pm 0.107687) \log k_{w, ODS} \quad (\text{Eq. 10})$$

where  $S = 0.111717$ ,  $R^2 = 0.8259$ ,  $F = 26.0903$ ,  $p = 0.000067$

$$\log K_p = -7.49410 (\pm 0.339119) + 0.51762 (\pm 0.133187) \log P_{average} + 0.0878685 (\pm 0.100416) \log k_{w,IAM} \quad (\text{Eq. 11})$$

where  $S = 0.113550$ ,  $R^2 = 0.8201$ ,  $F = 25.0787$ ,  $p = 0.000080$

Both QSAR equations (Eq. 10 and Eq. 11) could be further improved (Eq. 12 and Eq. 13) after removing three *ortho*-substituted molecules (**10**, **13** and **19**) as outliers:

$$\log K_p = -7.59071 (\pm 0.355353) + 0.440709 (\pm 0.285220) \log P_{average} + 0.200774 (\pm 0.281386) \log k_{w,ODS} \quad (\text{Eq. 12})$$

where  $S = 0.108514$ ,  $R^2 = 0.8792$ ,  $F = 29.1127$ ,  $p = 0.000213$

$$\log K_p = -7.48382 (\pm 0.442930) + 0.48975 (\pm 0.205593) \log P_{average} + 0.13816 (\pm 0.178504) \log k_{w,IAM} \quad (\text{Eq. 13})$$

where  $S = 0.107945$ ,  $R^2 = 0.8805$ ,  $F = 29.4629$ ,  $p = 0.000204$

Hence, the extrapolated retention parameters as chromatographic lipophilicity indices,  $\log k_{w,ODS}$  and  $\log k_{w,IAM}$  (derived with the linear model for acetonitrile-buffer systems on ODS and IAM columns) and computed  $\log P_{average}$  coefficients can be recommended to effectively assess the permeability of test molecules through the skin.

The significant linear correlations between the  $\log K_p$  coefficients and both chromatographic lipophilicity indices ( $\log k_{w,ODS}$  and  $\log k_{w,IAM}$ ) are shown in Figs S6A and B in Supplementary material. It was proven that the permeability through the skin of test molecules increases with their increasing lipophilicity indices. The more lipophilic analytes, possessing higher  $\log K_p$  coefficients, were assessed as better penetrating the skin due to the expected better absorption through the lipid bilayer of biomembranes.

In addition, the relationships between particular pharmacokinetic descriptors (*e.g.*  $\log K_{a,HSA}$ ,  $f_{u,brain}$ , Caco-2 and  $\log K_p$ ) predicted *in silico* and those obtained on the basis of Eqs 4-11 are shown (Figs S7-10 in Supplementary material) with square correlation coefficients ranging from 0.820 to 0.915.

#### 4. Conclusion

Two innovative and effective synthetic procedures (based on rational bioisosteric replacements) were developed, which allow preparing fourteen novel fused azaisocytosine-containing molecules belonging to two original classes (**9-16** and **17-22**). The structures of

obtained compounds were confirmed by spectroscopic studies and their standardised lipophilicity indices were determined experimentally. The promising bioisosteres revealed not only antiproliferative activities against tumour cells but additionally lower toxicities in non-tumoural (Vero) cells. It was proven that isosteric replacement of the ethyl group in anticancer active fused azaisocytosine-containing molecules by the trifluoromethyl or isopropyl group was advantageous due to the reduced toxicity towards normal cells of almost all the designed drug-like bioisosteres (9-17, 19-22). Of all the compounds, especially three bioisosteres bearing the trifluoromethyl moiety (10, 12 and 13) proved to be the most promising in terms of selectivity as they are less toxic to normal cells than pemetrexed. In addition, the molecule 12 resulted also able to induce apoptosis by increasing caspase-6 and -8 levels in tumour cells. Furthermore, it was proven that the majority of test molecules with the trifluoromethyl moiety are more selective than their counterparts with the isopropyl group. Additionally, most of fused azaisocytosine-containing congeners revealed better or comparable antihemolytic effects than that of ascorbic acid (9-17) and Trolox (9-15 and 17), in an *ex vivo* model of oxidative haemolysis of rat erythrocytes. This significant finding proved that they are safe to red blood cells. In turn, the standardised  $\log k_w$  indices and  $\log P_{\text{average}}$  values were successfully used to derive statistically significant QSAR equations describing binding affinity to human serum albumin, fraction unbound (*e.g.* active) in brain tissue as well as effective jejunum and skin permeability in terms of lipophilicity parameters of test bioisosteres with relevance in human medicine.

The representatives of two novel classes which are the least toxic for normal cells, deprived of hemolytic effects on oxidatively-stressed red blood cells and revealing the optimum pharmacokinetic descriptors in terms of their lipophilicity indices, may be regarded as possible drug-like candidates (with the applicability potential in human solid tumours). They may be utilised in further more extended *in vivo* investigations aimed at developing novel less toxic anticancer agents.

### **Conflict of interest**

The authors declare no conflict of interest.

### **Appendix A. Supplementary data**

Supplementary data to this article can be found online.

### **References**

- [1] M.S. Apro, Innovative metabolites in solid tumours, Springer-Verlag Berlin, Heidelberg, 1994.
- [2] L-C. Hwang, C.-J. Wang, G.-H. Lee, Y. Wang, C.-C. Tzeng, Synthesis and structure assignment of 1-[(2-hydroxy-ethoxymethyl)- and 1-[(1,3-dihydroxy-2-propoxymethyl)-6-azaisocytosine, Heterocycles 41 (1995) 293-301.
- [3] E. Kaminskas, A.T. Farrell, Y.-Ch. Wang, R. Sridhara, R. Pazdur, FDA drug approval summary: azacitidine (5-azacytidine, Vidaza™) for injectable suspension, Oncologist 10 (2005) 176-182.
- [4] M. Sztanke, J. Rzymowska, M. Janicka, K. Sztanke, Synthesis, structure elucidation, determination of antiproliferative activities, lipophilicity indices and pharmacokinetic properties of novel fused azaisocytosine-like congeners, Arab. J. Chem. (2016) <http://dx.doi.org/10.1016/j.arabjc.2016.04.002>.
- [5] M. Sztanke, J. Rzymowska, M. Janicka, K. Sztanke, Synthesis, structure confirmation, identification of *in vitro* antiproliferative activities and correlation of determined lipophilicity parameters with *in silico* bioactivity descriptors of two novel classes of fused azaisocytosine-like congeners, Arab. J. Chem. (2017) <http://dx.doi.org/10.1016/j.arabjc.2016.12.024>.
- [6] K. Sztanke, J. Rzymowska, M. Niemczyk, I. Dybała, A.E. Koziół, Synthesis, crystal structure and anticancer activity of novel derivatives of ethyl 1-(4-oxo-8-aryl-4,6,7,8-tetrahydroimidazo[2,1-*c*][1,2,4]triazin-3-yl)formate, Eur. J. Med. Chem. 41 (2006) 539-547.
- [7] K. Sztanke, K. Pasternak, J. Rzymowska, M. Sztanke, M. Kandfer-Szerszeń, Synthesis, structure elucidation and identification of antitumoural properties of novel fused 1,2,4-triazine aryl derivatives, Eur. J. Med. Chem. 43 (2008) 1085-1094.
- [8] K. Sztanke, K. Pasternak, M. Sztanke, M. Kandfer-Szerszeń, A.E. Koziół, I. Dybała, Crystal structure, antitumour and antimetastatic activities of disubstituted fused 1,2,4-triazinones, Bioorg. Med. Chem. Lett. 19 (2009) 5095-5100.
- [9] K. Sztanke, T. Tuzimski, M. Sztanke, J. Rzymowska, K. Pasternak, Synthesis, structure elucidation, determination of the lipophilicity and identification of antitumour activities *in vitro* of novel 3-(2-furanyl)-8-aryl-7,8-dihydroimidazo[2,1-*c*][1,2,4]triazin-4(6*H*)-ones with a low cytotoxicity towards normal human skin fibroblast cells, Bioorg. Med. Chem. 19 (2011) 5103-5116.

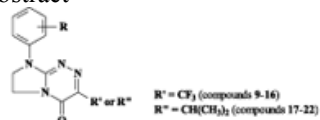
- [10] M. Sztanke, J. Rzymowska, K. Sztanke, Synthesis, structure elucidation and *in vitro* anticancer activities of novel derivatives of diethyl (2*E*)-2-[(2*E*)-(1-arylimidazolidin-2-ylidene)hydrazono]succinate and ethyl (4-oxo-8-aryl-4,6,7,8-tetrahydroimidazo[2,1-*c*][1,2,4]triazin-3-yl)acetate, *Bioorg. Med. Chem.* 21 (2013) 7465-7480.
- [11] M. Sztanke, J. Rzymowska, K. Sztanke, Synthesis, structure elucidation and identification of antiproliferative activities of a novel class of thiophene bioisosteres bearing the privileged 7,8-dihydroimidazo[2,1-*c*][1,2,4]triazin-4(6*H*)-one scaffold, *Bioorg. Med. Chem.* 23 (2015) 3448-3456.
- [12] M. Sztanke, T. Tuzimski, M. Janicka, K. Sztanke, Structure-retention behaviour of biologically active fused 1,2,4-triazinones – Correlation with *in silico* molecular properties, *Eur. J. Pharm. Sci.* 68 (2015) 114-126.
- [13] M. Sztanke, K. Sztanke, B. Rajtar, Ł. Świątek, A. Boguszewska, M. Polz-Dacewicz, The influence of some promising fused azaisocytosine-containing congeners on zebrafish (*Danio rerio*) embryos/larvae and their antihaemolytic, antitumour and antiviral activities, *Eur. J. Pharm. Sci.* 132 (2019) 34-43.
- [14] M. Janicka, M. Sztanke, K. Sztanke, Reversed-phase liquid chromatography with octadecylsilyl, immobilized artificial membrane and cholesterol columns in correlation studies with *in silico* biological descriptors of newly synthesized antiproliferative and analgesic active compounds, *J. Chromatogr. A* 1318 (2013) 92-101.
- [15] J. Pitha, P. Fiedler, J. Gut, Nucleic acids components and their analogues. LXXXII. The fine structure of 6-azaisocytosine and its derivatives, *Collect. Czech. Chem. Commun.* 31 (1966) 1864-1871.
- [16] R. Łyszczek, A. Bartyzel, H. Głuchowska, L. Mazur, M. Sztanke, K. Sztanke, Thermal investigations of biologically important fused azaisocytosine-containing congeners and the crystal structure of one representative, *J. Anal. Appl. Pyrolysis* 135 (2018) 141-151.
- [17] S. Taliani, I. Pugliesi, E. Barresi, F. Simorini, S. Salerno, C. La Motta, A.M. Marini, B. Cosimelli, S. Cosconati, S. Di Maro, L. Marinelli, S. Daniele, M.L. Trincavelli, G. Greco, E. Novellino, C. Martini, F. Da Settimo, 3-Aryl-[1,2,4]triazino[4,3-*a*]benzimidazol-4(10*H*)-one: A novel template for the design of highly selective A<sub>2B</sub> adenosine receptor antagonists, *J. Med. Chem.* 55 (2012) 1490-1499.
- [18] M. Sztanke, J. Rzymowska, K. Sztanke, *In vitro* effects of a new fused azaisocytosine-like congener on relative cell proliferation, necrosis and cell cycle in cancer and normal cell cultures. *Mol. Cell. Biochem.* 418 (2016) 179-188.

- [19] A. Szuster-Ciesielska, K. Sztanke, M. Kandefer-Szerszeń, A novel fused 1,2,4-triazine aryl derivative as antioxidant and nonselective antagonist of adenosine A<sub>2A</sub> receptors in ethanol-activated liver stellate cells, *Chem. Biol. Interact.* 195 (2012) 18-24.
- [20] M. Sztanke, K. Sztanke, inventors; Medical University of Lublin, assignee, 3-Ethyl-8-aryl-7,8-dihydroimidazo[2,1-*c*][1,2,4]triazin-4(6*H*)-ones, method for obtaining them and medical applications, Polish Patent 224679, 2017.
- [21] K. Sztanke, J. Rzymowska, M. Niemczyk, I. Dybała, A.E. Koziół, Novel derivatives of methyl and ethyl 2-(4-oxo-8-aryl-2*H*-3,4,6,7-tetrahydroimidazo[2,1-*c*][1,2,4]triazin-3-yl)acetates from biologically active 1-aryl-2-hydrazinoimidazolines: synthesis, crystal structure and antiproliferative activity, *Eur. J. Med. Chem.* 41 (2006) 1373-1384.
- [22] K. Sztanke, inventor; Medical University of Lublin, assignee, New 1-substituted-2-hydrazino-4,5-dihydroimidazole hydroiodides and method for their obtaining, Polish Patent 211550, 2012.
- [23] R. Kaliszan, QSRR: Quantitative structure-(chromatographic) retention relationships, *Chem. Rev.* 107 (2007) 3212-3246.
- [24] M. Sztanke, K. Sztanke, Derivatives of 3-(trifluoromethyl)-7,8-dihydroimidazo[2,1-*c*][1,2,4]triazin-4(6*H*)-one substituted by phenyl, alkylphenyl and alkoxyphenyl, method for obtaining them and medical application, Patent Application Publication No: PL 2019/429161 A1, 2019.
- [25] M. Sztanke, K. Sztanke, 3-(Trifluoromethyl)-7,8-dihydroimidazo[2,1-*c*][1,2,4]triazin-4(6*H*)-ones substituted by monochlorophenyl or dichlorophenyl, method for obtaining them and medical application, Patent Application Publication No: PL 2019/429162 A1, 2019.
- [26] M. Sztanke, K. Sztanke, 8-Substituted-3-(propan-2-yl)-7,8-dihydroimidazo[2,1-*c*][1,2,4]triazin-4(6*H*)-ones, method for obtaining them and medical application, Patent Application Publication No: PL 2019/429163 A1, 2019.
- [27] R.B. Badisa, S.F. Darling-Reed, P. Joseph, J.S. Cooperwood, L.M. Latinwo, C.B. Goodman, Selective cytotoxic activities of two novel synthetic drugs on human breast carcinoma MCF-7 cells, *Anticancer Res.* 29 (2009) 2993-2996.
- [28] J. Moreira, D. Ribeiro, P.M.A. Silva, N. Nazareth, M. Monteiro, A. Palmeira, L. Saraiva, M. Pinto, H. Bousbaa, H. Cidade, New alkoxy flavone derivatives targeting caspases: synthesis and antitumor activity evaluation, *Molecules* 24 (2019) 129.
- [29] S. Shalini, L. Dorstyn, S. Dawar, S. Kumar, Old, new and emerging functions of caspases, *Cell Death Differ.* 22 (2015) 526-539.

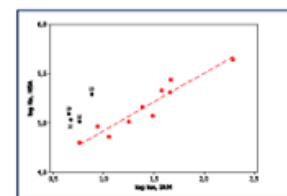
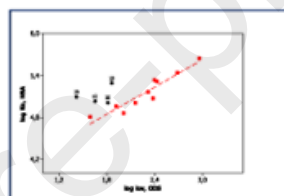
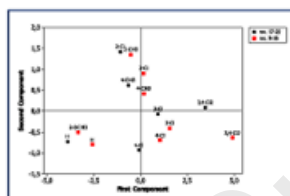
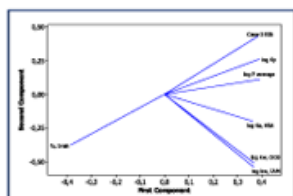
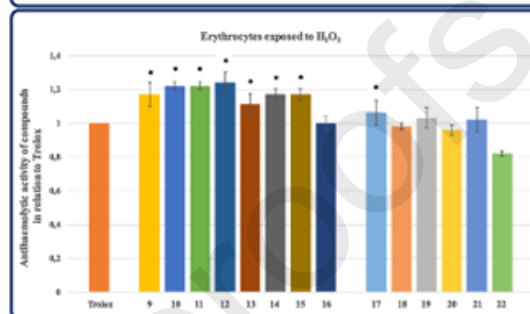
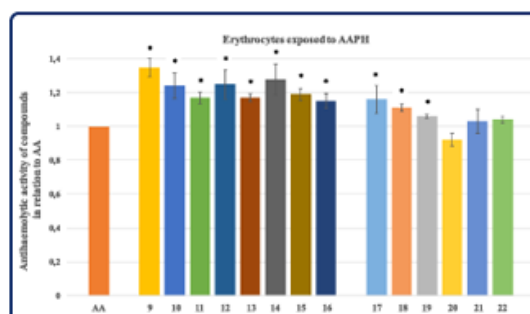
- [30] S. Patel, P. Modi, V. Ranjan, M. Chhabria, Structure-based design, synthesis and evaluation of 2,4-diaminopyrimidine derivatives as novel caspase-1 inhibitors, *Bioorg. Chem.* 78 (2018) 258-268.
- [31] M.F. Mohamed, N. Samir, A. Ali, N. Ahmed, Y. Ali, S. Aref, O. Hossam, M.S. Mohamed, A.M. Abdelmoniem, I.A. Abdelhamid, Apoptotic induction mediated p53 mechanism and caspase-3 activity by novel promising cyanoacrylamide derivatives in breast carcinoma, *Bioorg. Chem.* 73 (2017) 43-52.
- [32] E. Soczewiński, C.A. Wachtmeister, The relation between the composition of certain ternary two-phase solvent systems and RM values, *J. Chromatogr.* 7 (1962) 311-320.
- [33] K. Valko, Application of high-performance liquid chromatography based measurements of lipophilicity to model biological distribution, *J. Chromatogr. A* 1037 (2004) 299-310.
- [34] C. Binkert, M. Frigerio, A. Jones, S. Meyer, C. Pesenti, L. Prade, F. Viani, M. Zanda, Replacement of isobutyl by trifluoromethyl in pepstatin A selectively affects inhibition of aspartic proteinases, *ChemBioChem* 7 (2006) 181-186.
- [35] M.M. Hsieh, J.G. Dorsey, Accurate determination of log  $k'_w$  in reversed-phase liquid chromatography. Implications for quantitative structure-retention relationships, *J. Chromatogr.* 631 (1993) 63-78.
- [36] W.J. Lambert, Modeling oil-water partitioning and membrane permeation using reversed-phase chromatography, *J. Chromatogr. A* 656 (1993) 469-484.
- [37] P.A. Carrupt, B. Testa, P. Gaillard, Computational approaches to lipophilicity: methods and applications, Chapter 5, in: K.B. Lipkowitz, D.B. Boyd, (Eds.), *Reviews in Computational Chemistry*, Volume 11, Wiley-VCH, J. Wiley and Sons Inc., New York, 1997.
- [38] N. Perisic-Janjic, R. Kaliszan, N. Milosevic, G. Uscumlic, N. Banjac, Chromatographic retention parameters in correlation analysis with in silico biological descriptors of a novel series of N-phenyl-3-methyl succinimide derivatives, *J. Pharm. Biomed. Anal.* 72 (2013) 65-73.
- [39] R. Kaliszan, A. Nasal, M. Turowski, Quantitative structure-retention relationships in the examination of the topography of the binding site of antihistamine drugs on  $\alpha_1$ -acid glycoprotein, *J. Chromatogr. A* 722 (1996) 25-32.
- [40] A. Nasal, A. Radwańska, K. Ośmiałowski, A. Buciąński, R. Kaliszan, R. Barker, P. Sun, R.A. Hartwick, Quantitative relationships between the structure of beta-adrenolytic and antihistamine drugs and their retention on an alpha 1-acid glycoprotein HPLC column, *Biomed. Chromatogr.* 8 (1994) 125-129.

- [41] F. Barbato, V. Cirocco, L. Grumetto, M.I. La Rotonda, Comparison between immobilized artificial membrane (IAM) HPLC data and lipophilicity in *n*-octanol for quinolone antibacterial agents, *Eur. J. Pharm. Sci.* 31 (2007) 288-297.
- [42] M. Janicka, A. Pachuta-Stec, Retention-property relationships of 1,2,4-triazoles by micellar and reversed-phase liquid chromatography, *J. Sep. Sci.* 37 (2014) 1419-1428.
- [43] S. Yamashita, T. Furubayashi, M. Kataoka, T. Sakane, H. Sezaki, H. Tokuda, Optimized conditions for prediction of intestinal drug permeability using Caco-2 cells, *Eur. J. Pharm.* 10 (2000) 195-204.
- [44] M. Yazdanian, S.L. Glynn, J.L. Wright, A. Hawi, Correlating partitioning and Caco-2 cell permeability of structurally diverse small molecular weight compounds, *Pharm. Res.* 15 (1998) 1490-1494.

## Graphical abstract



R	Incubation time	Selectivity indices					
		A549		T47D		HeLa	
		R'	R''	R'	R''	R'	R''
H	24 h	~1.00	~1.00	~1.00	~1.00	~1.00	> 1.00
	48 h	< 1.00	~1.00	1.64	> 1.39	1.00	> 1.39
	72 h	0.83	< 1.00	1.67	1.80	1.36	1.80
2-CH <sub>3</sub>	24 h	~1.00		~1.00		~1.00	
	48 h	~1.00		> 1.64		> 1.20	
	72 h	> 1.29		> 2.00		> 1.64	
4-CH <sub>3</sub>	24 h	~1.00	~1.00	~1.00	> 1.00	~1.00	~1.00
	48 h	> 1.20	< 0.72	> 1.64	1.08	> 1.29	1.00
	72 h	1.55	< 0.56	1.89	1.11	1.70	1.00
2-OCH <sub>3</sub>	24 h	~1.00		~1.00		~1.00	
	48 h	> 1.29		> 2.00		> 1.00	
	72 h	> 1.80		> 2.00		> 2.00	
2-Cl	24 h	~1.00	~1.00	~1.00	~1.00	~1.00	> 1.39
	48 h	~1.00	~1.00	> 1.64	> 1.39	~1.00	> 1.80
	72 h	> 1.50	> 1.29	> 2.00	> 1.80	> 1.64	> 2.00
3-Cl	24 h	~1.00	~1.00	~1.00	~1.00	~1.00	~1.00
	48 h	> 1.39	-1.00	> 1.64	> 1.29	> 1.00	> 1.50
	72 h	2.00	1.00	2.00	1.89	1.50	1.70
4-Cl	24 h	~1.00	~1.00	~1.00	~1.00	~1.00	~1.00
	48 h	~1.00	~1.00	> 1.64	> 1.29	> 1.39	> 1.13
	72 h	1.29	> 1.29	2.00	> 2.00	2.00	> 1.64
3,4-Cl <sub>2</sub>	24 h	~1.00	~1.00	~1.00	~1.00	~1.00	~1.00
	48 h	> 1.39	> 1.06	> 2.00	> 1.80	> 1.50	> 1.39
	72 h	1.56	1.15	1.56	1.67	1.56	1.50
Pemetrexed	24 h	~1.00		~1.00		~1.00	
	48 h	~1.00		~1.00		> 1.00	
	72 h	> 1.00		~1.00		> 1.20	

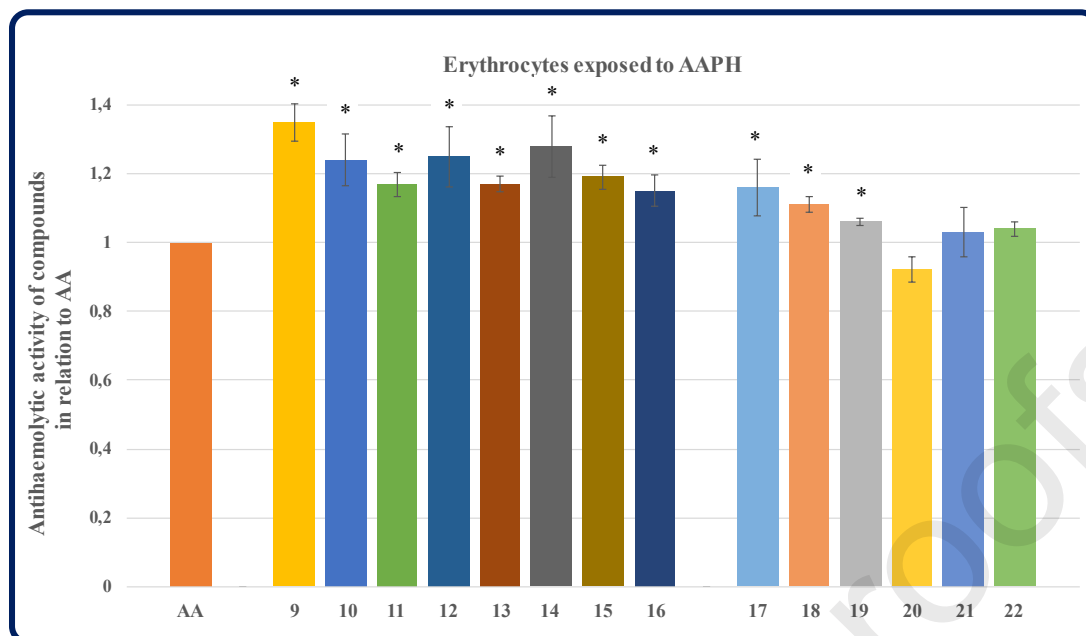


**Highlights**

- Novel heteroannulation routes leading to new congeneric classes have been developed
- Most of compounds are higher cytotoxic than pemetrexed for human tumour cells
- Structures **10**, **12**, **13** are less or equally toxic to Vero cells as pemetrexed
- Most of molecules evoked protective effects on oxidatively-stressed erythrocytes
- Correlations of logs *k* vs. *in silico* pharmacokinetic descriptors are significant

Journal Pre-proofs

A



B

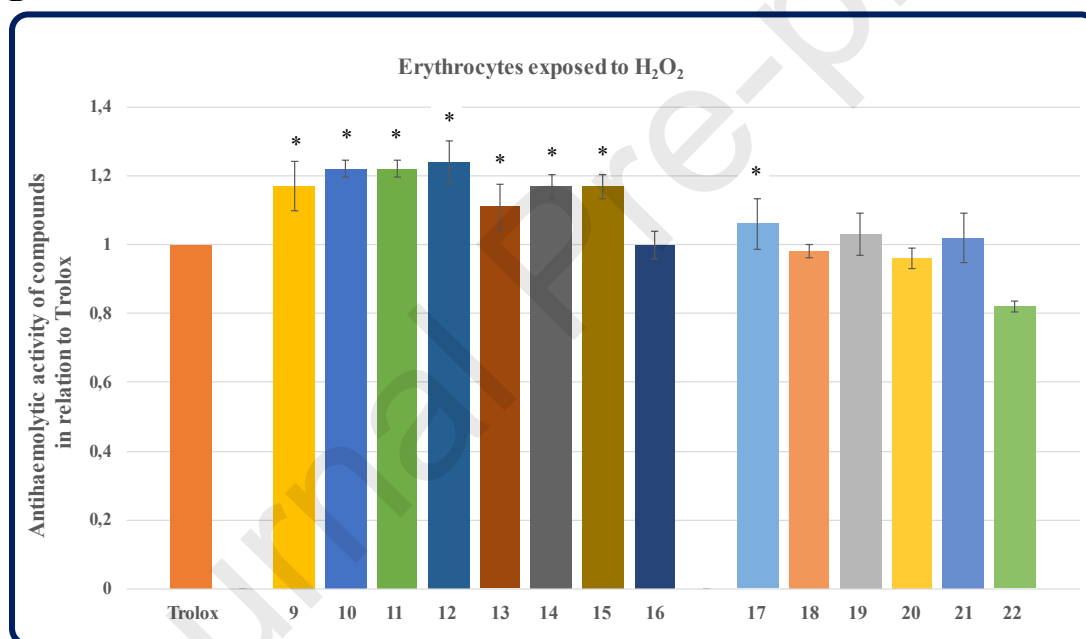


**Fig. 1.** Antihæmolytic activities (in the model of rat erythrocytes exposed to AAPH) of fused azaisocytosine-containing congeners (**9-22**) in relation to ascorbic acid (**A**). Antihæmolytic activities (in the model of rat erythrocytes exposed to H<sub>2</sub>O<sub>2</sub>) of fused azaisocytosine-containing congeners (**9-22**) in relation to Trolox (**B**). Compounds and standard drugs (AA and Trolox) were tested at a concentration of 200 µM.

AAPH – 2,2'-azobis(2-methylpropionamide) dihydrochloride; AA – ascorbic acid; H<sub>2</sub>O<sub>2</sub> – hydrogen peroxide; Trolox – 6-hydroxy-2,5,7,8-tetramethylchroman-2-carboxylic acid.

Data (from four independent experiments) are shown as the mean ± standard deviation.

\* – the activity of compound statistically significantly higher than that of a positive control ( $p < 0.05$ , Student's *t*-test)

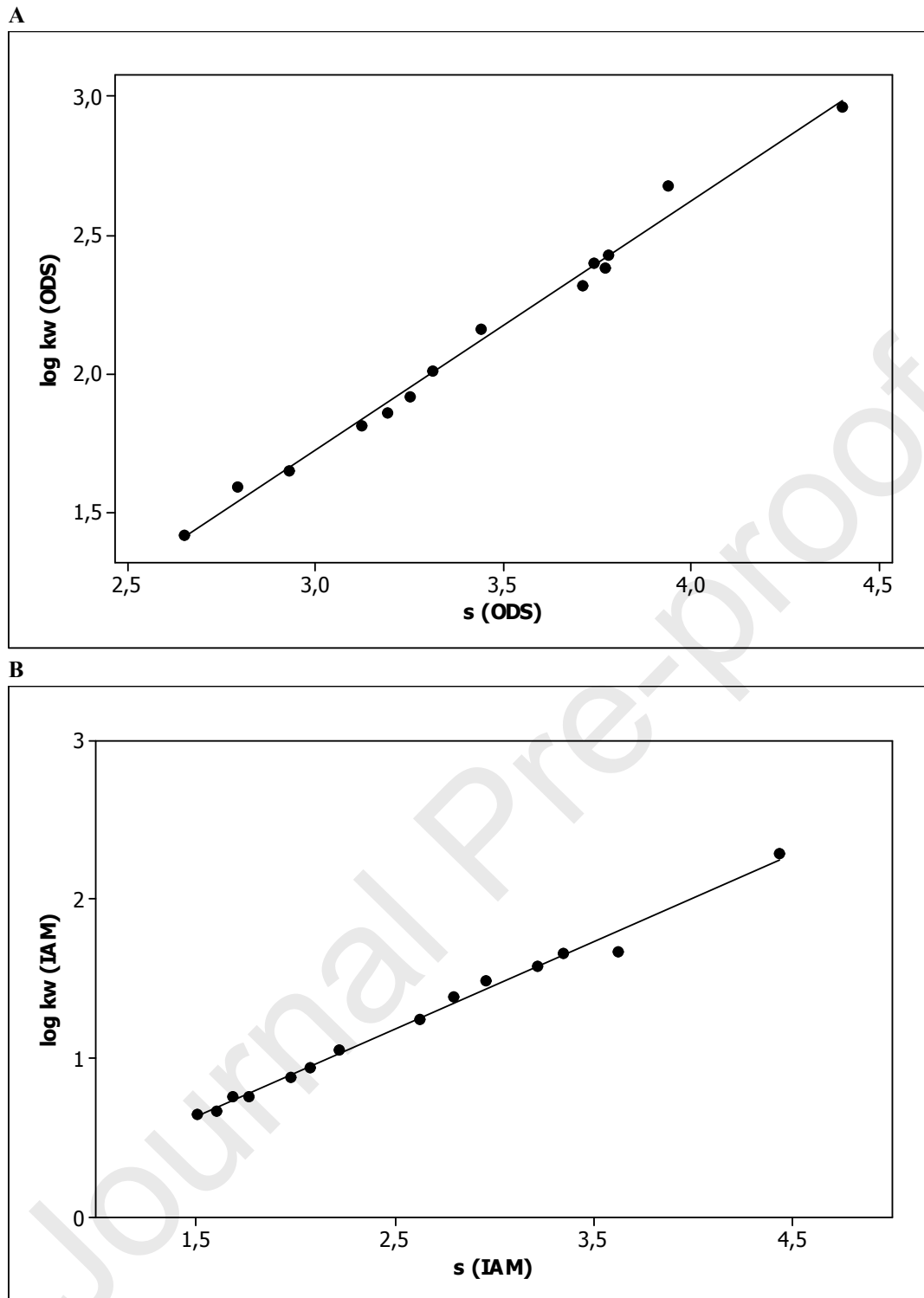


**Fig. 2.** The relationship between  $\log k_{w, ODS}$  and  $s_{ODS}$  values (**A**). The relationship between  $\log k_{w, IAM}$  and  $s_{IAM}$  values (**B**).

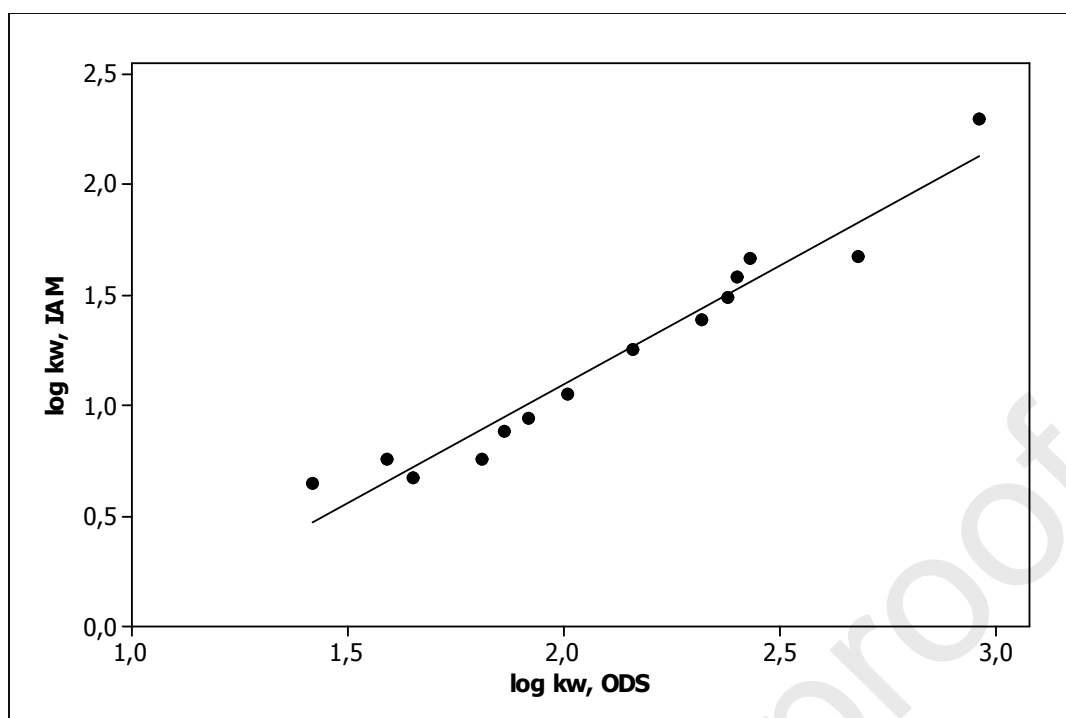


**Fig. 3.** The correlation between  $\log k_{w, \text{IAM}}$  and  $\log k_{w, \text{ODS}}$ . The  $\log k_w$  values were calculated by linear extrapolation based on the experimental data obtained for the IAM and ODS columns according to the equation of Soczewiński-Wachtmeister.

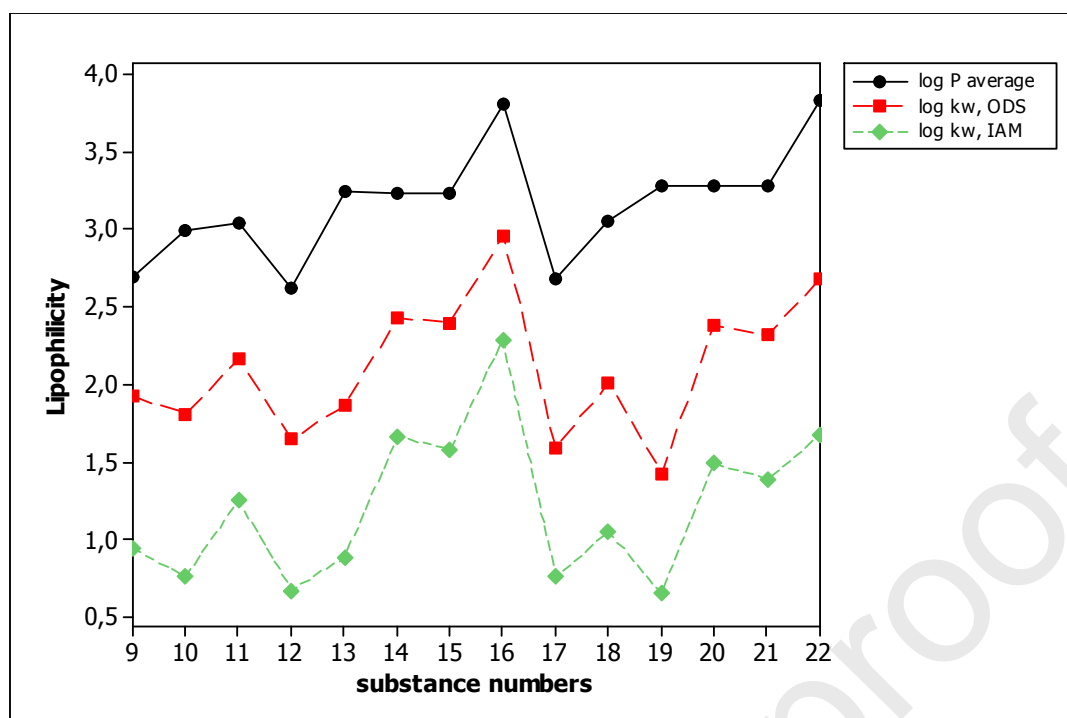
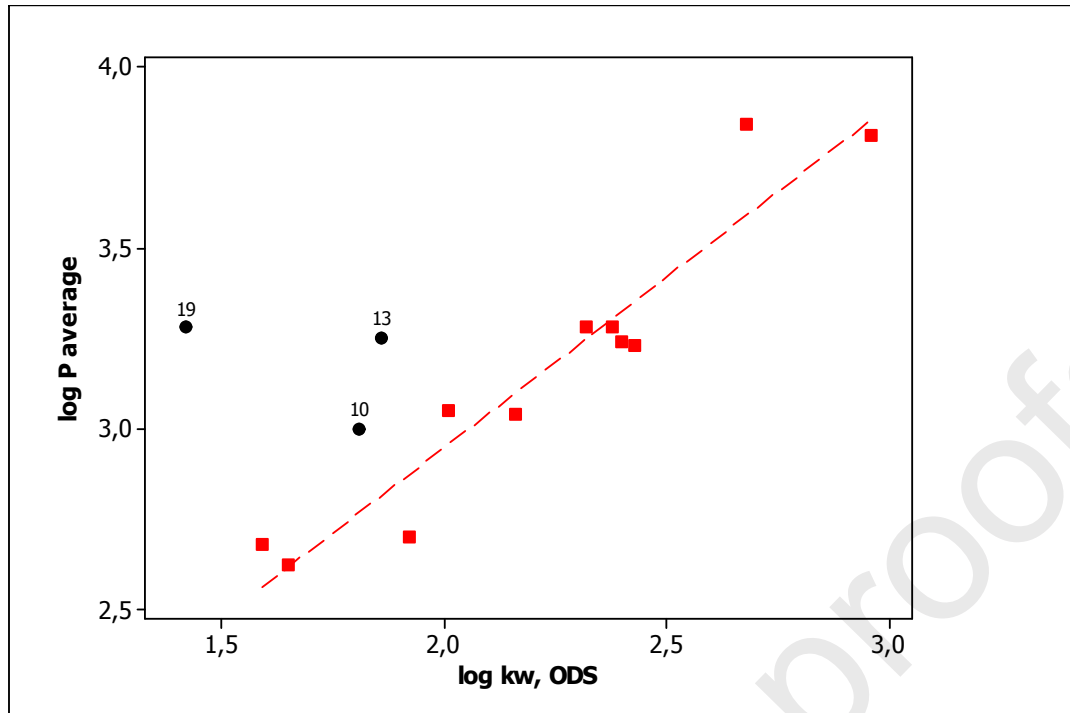


**Fig. 4.** Lipophilicity profiles of the studied compounds that were computed and determined experimentally using two different stationary phases.

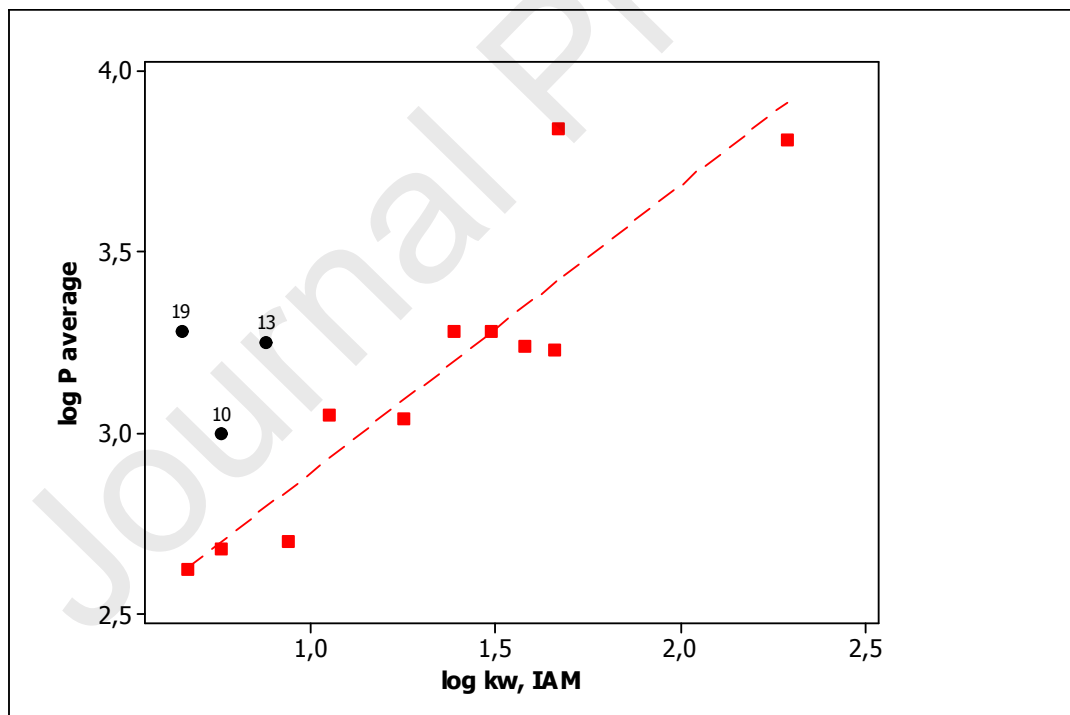
A



$$\log P_{average} = 1.0602 (\pm 0.2181) + 0.94320 (\pm 0.09641) \log k_{w,ODS}$$

$$S = 0.126819, R^2 = 0.914, F = 95.71, p = 0.000$$

B



$$\log P_{average} = 2.0963 (\pm 0.1656) + 0.7940 (\pm 0.1171) \log k_{w,IAM}$$

$$S = 0.175014, R^2 = 0.836, F = 45.98, p = 0.000$$

**Fig. 5.** The relationship between  $\log P_{average}$  and  $\log k_{w, ODS}$  values (**A**). The relationship between  $\log P_{average}$  and  $\log k_{w, IAM}$  values (**B**).

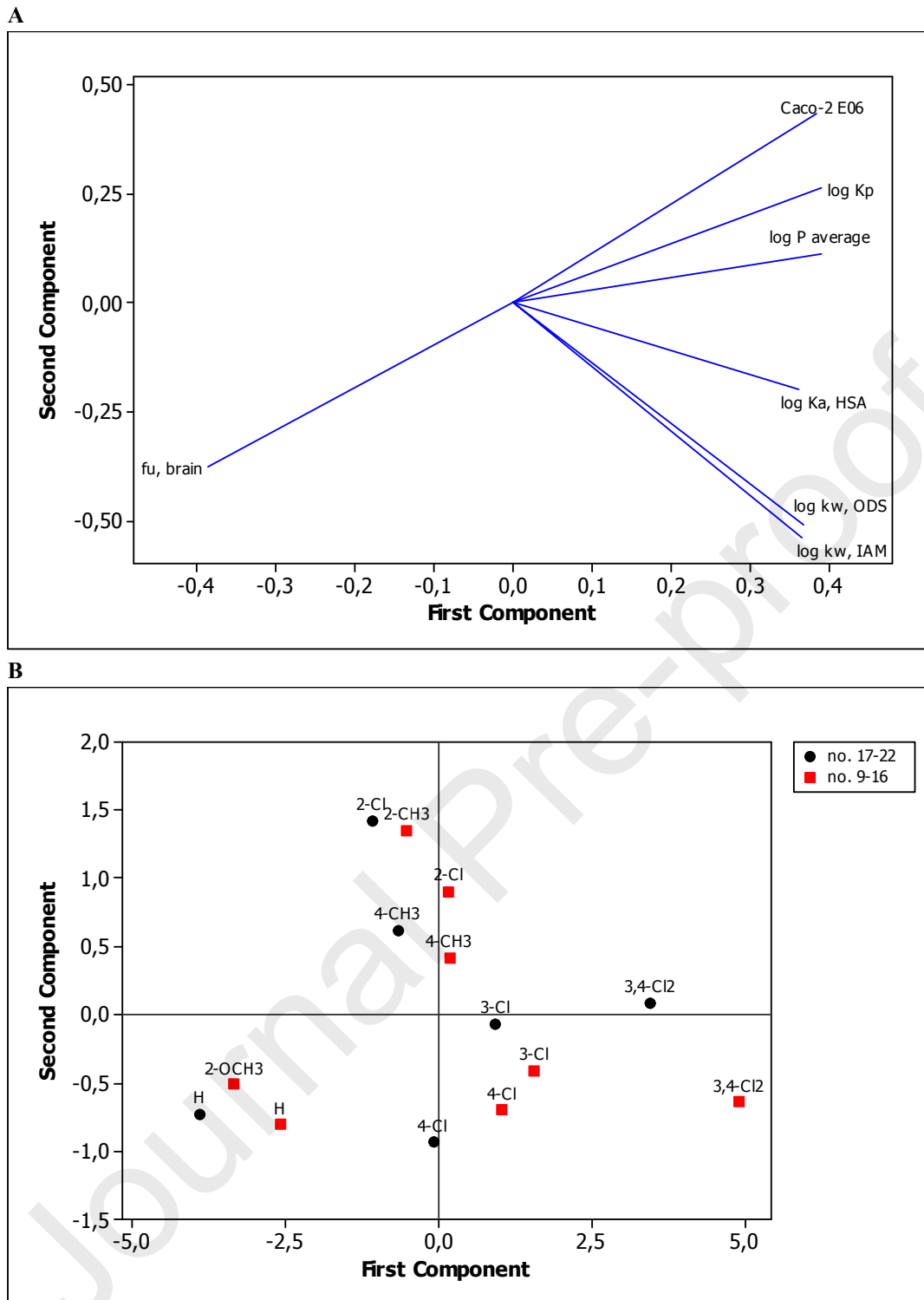
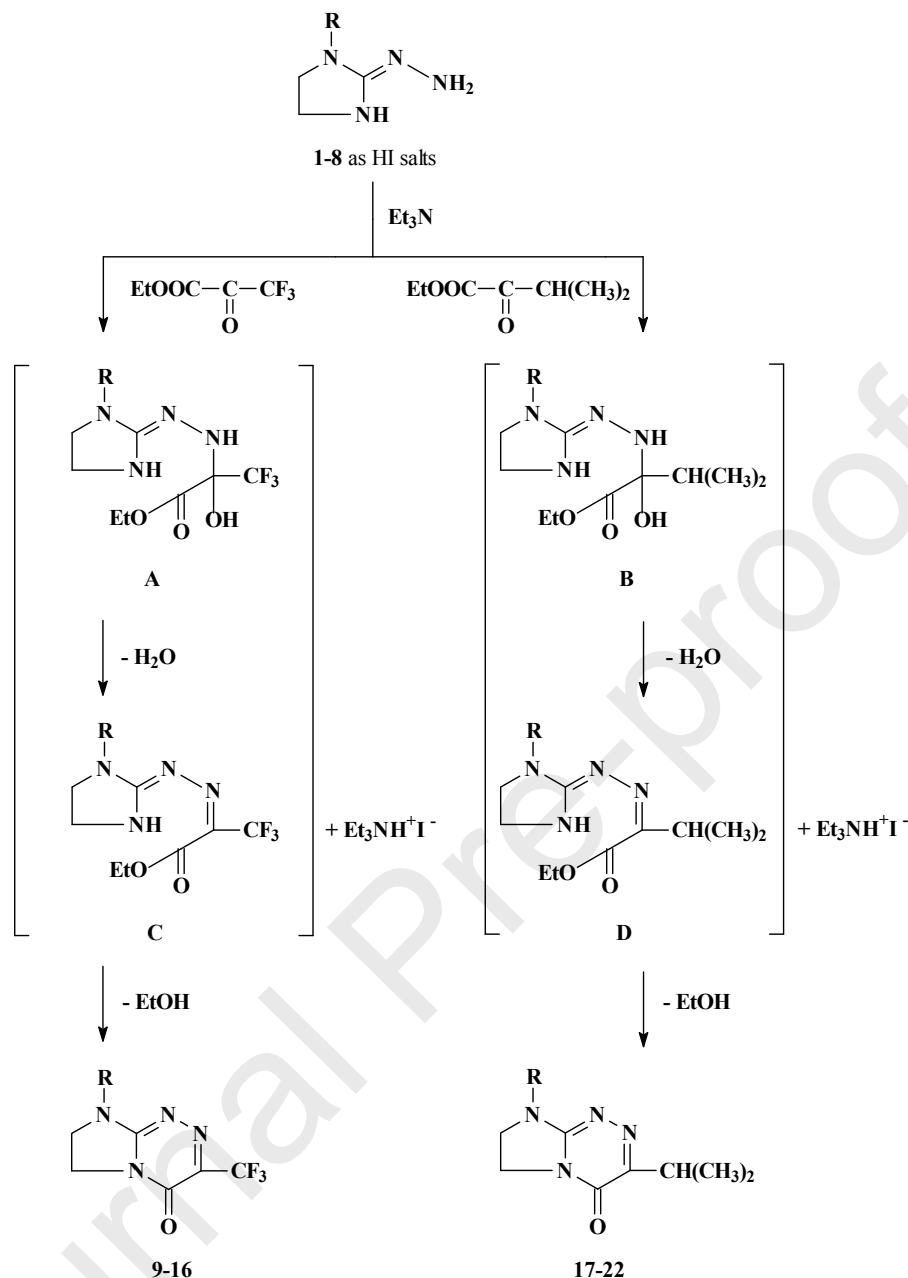


**Fig. 6.** The loading plot of  $\log P_{average}$ , Caco-2,  $\log K_p$ ,  $\log k_w$ , ODS,  $\log K_a$  HSA,  $\log k_w$ , IAM, fu, brain (A). The score plot of PC2 versus PC1 (B).



**Scheme 1.** Synthesis of compounds belonging to the trifluoromethyl (**9-16**) and isopropyl (**17-22**) series. **1, 9, 17:** R = C<sub>6</sub>H<sub>5</sub>; **2, 10:** R = 2-CH<sub>3</sub>C<sub>6</sub>H<sub>4</sub>; **3, 11, 18:** R = 4-CH<sub>3</sub>C<sub>6</sub>H<sub>4</sub>; **4, 12:** R = 2-OCH<sub>3</sub>C<sub>6</sub>H<sub>4</sub>; **5, 13, 19:** R = 2-ClC<sub>6</sub>H<sub>4</sub>; **6, 14, 20:** R = 3-ClC<sub>6</sub>H<sub>4</sub>; **7, 15, 21:** R = 4-ClC<sub>6</sub>H<sub>4</sub>; **8, 16, 22:** R = 3,4-Cl<sub>2</sub>C<sub>6</sub>H<sub>3</sub>.

**Table 1**Cytotoxicity of the investigated fused azaisocytosine-containing congeners (**9-22**) in non-tumoural and tumour cells.

Compound	R	Incubation time	Cytotoxicity expressed as growth inhibition (%) in cell lines			
			Vero	A549	T47D	HeLa
<b>9</b>	H	24 h	30 ± 0.9	2 ± 0.2	35 ± 1.5	20 ± 0.8
		48 h	50 ± 0.8	25 ± 1.4	80 ± 4.8	50 ± 1.8
		72 h	60 ± 1.2	50 ± 2.5	100 ± 6.8	80 ± 4.6
<b>10</b>	2-CH <sub>3</sub>	24 h	2 ± 0.1	5 ± 0.9	21 ± 1.2	16 ± 0.8
		48 h	10 ± 0.6	36 ± 2.6	78 ± 3.6	57 ± 2.6
		72 h	26 ± 0.7	62 ± 2.0	99 ± 5.8	83 ± 4.6
<b>11</b>	4-CH <sub>3</sub>	24 h	10 ± 0.4	26 ± 1.7	10 ± 1.3	21 ± 1.3
		48 h	42 ± 1.3	57 ± 2.6	83 ± 5.4	62 ± 3.8
		72 h	52 ± 1.6	78 ± 2.9	100 ± 5.8	89 ± 5.7
<b>12</b>	2-OCH <sub>3</sub>	24 h	2 ± 0.3	22 ± 1.0	22 ± 1.8	17 ± 1.5
		48 h	11 ± 0.8	61 ± 2.6	94 ± 5.3	50 ± 2.8
		72 h	33 ± 0.7	88 ± 3.9	100 ± 5.0	99 ± 5.0
<b>13</b>	2-Cl	24 h	6 ± 0.9	17 ± 0.9	28 ± 1.6	11 ± 0.7
		48 h	11 ± 0.7	33 ± 2.7	84 ± 6.5	45 ± 2.2
		72 h	22 ± 0.9	72 ± 3.1	100 ± 3.6	78 ± 4.0
<b>14</b>	3-Cl	24 h	17 ± 1.0	28 ± 1.8	17 ± 1.3	11 ± 0.6
		48 h	22 ± 0.7	67 ± 3.1	84 ± 5.8	50 ± 2.7
		72 h	50 ± 1.3	95 ± 5.0	100 ± 7.2	72 ± 3.6
<b>15</b>	4-Cl	24 h	22 ± 0.6	6 ± 0.9	28 ± 1.3	11 ± 0.7
		48 h	39 ± 0.9	17 ± 1.3	78 ± 3.9	67 ± 3.1
		72 h	50 ± 1.6	61 ± 2.8	100 ± 6.5	100 ± 5.8
<b>16</b>	3,4-Cl <sub>2</sub>	24 h	19 ± 1.0	37 ± 1.4	25 ± 1.1	6 ± 0.3
		48 h	43 ± 1.9	68 ± 3.5	100 ± 7.2	74 ± 3.2
		72 h	62 ± 2.2	100 ± 5.6	100 ± 7.7	100 ± 6.7
<b>17</b>	H	24 h	9 ± 0.5	9 ± 0.4	9 ± 0.5	50 ± 1.4
		48 h	41 ± 1.6	18 ± 0.6	68 ± 5.0	68 ± 4.1
		72 h	50 ± 1.1	27 ± 1.0	86 ± 2.5	90 ± 6.8
<b>18</b>	4-CH <sub>3</sub>	24 h	48 ± 4.3	2 ± 0.5	48 ± 2.7	43 ± 3.2
		48 h	67 ± 5.9	10 ± 0.6	76 ± 3.4	67 ± 4.0
		72 h	86 ± 5.2	24 ± 1.1	95 ± 5.5	86 ± 3.4
<b>19</b>	2-Cl	24 h	10 ± 0.4	20 ± 0.5	10 ± 0.8	67 ± 4.7
		48 h	31 ± 0.8	31 ± 1.5	67 ± 2.6	87 ± 3.9
		72 h	46 ± 0.9	61 ± 1.1	92 ± 4.9	97 ± 5.3
<b>20</b>	3-Cl	24 h	20 ± 0.2	26 ± 0.7	20 ± 0.8	26 ± 0.9
		48 h	46 ± 1.1	31 ± 1.2	61 ± 2.7	72 ± 3.6
		72 h	51 ± 1.2	51 ± 1.5	100 ± 4.9	92 ± 5.9
<b>21</b>	4-Cl	24 h	10 ± 0.5	5 ± 0.4	10 ± 0.5	20 ± 1.4
		48 h	31 ± 0.9	20 ± 0.8	61 ± 2.7	56 ± 3.6
		72 h	46 ± 1.4	61 ± 2.3	97 ± 5.7	77 ± 3.3
<b>22</b>	3,4-Cl <sub>2</sub>	24 h	23 ± 0.6	11 ± 0.6	23 ± 1.4	11 ± 0.7
		48 h	34 ± 0.7	51 ± 1.8	91 ± 6.3	69 ± 3.2
		72 h	57 ± 1.8	69 ± 3.2	100 ± 6.7	86 ± 4.8
Standard drug		24 h	5 ± 0.3	15 ± 0.9	5 ± 0.4	15 ± 1.2
		48 h	20 ± 1.2	30 ± 1.8	15 ± 0.7	50 ± 2.5
		72 h	25 ± 1.4	50 ± 3.2	25 ± 0.9	60 ± 4.5

Non-tumoural cell line: Vero – (ECACC 88020401) – African Green Monkey kidney cells

Cancer cell lines: A549 (ECACC 86012804) – human Caucasian lung carcinoma cells; T47D (ECACC 85102201) – human breast carcinoma cells; HeLa (ECACC 93021013) – human Negroid cervix epitheloid carcinoma cells

The standard drug – pemetrexed at a concentration of 0.176 mM

Compounds were tested at a concentration of 0.176 mM.

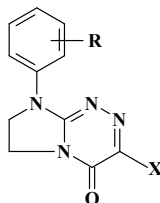
Data (from five independent experiments) are shown as the mean  $\pm$  standard deviation.

Growth inhibition (%) =  $100 - [(Abs_{\text{sample}} - Abs_{\text{blank}}) / (Abs_{\text{control}} - Abs_{\text{blank}})] \times 100$ , where  $Abs_{\text{sample}}$  denotes the absorbance of sample with the test compound,  $Abs_{\text{control}}$  denotes the absorbance of sample without the test compound,  $Abs_{\text{blank}}$  denotes the absorbance of distilled water.

Journal Pre-proofs

**Table 2**

Comparison of cytotoxicities *in vitro* towards non-tumoural cells of the epithelial origin for the previously described fused azaisocytosine-containing nucleobases with ethyl substituent [5] and the corresponding counterparts with the trifluoromethyl and isopropyl groups (comparable in terms of steric effect).



R	Incubation period	Cytotoxicity expressed as growth inhibition (%) in Vero cell line		
		X = Et <sup>a</sup>	X = CF <sub>3</sub>	X = iPr
H	24-h	50 ± 4.2	30 ± 0.9	10 ± 0.6
	48-h	60 ± 5.5	<b>9</b> 50 ± 0.8	<b>17</b> 45 ± 1.8
	72-h	90 ± 8.6	60 ± 1.2	55 ± 1.2
4-CH <sub>3</sub>	24-h	50 ± 3.5	10 ± 0.4	50 ± 4.5
	48-h	60 ± 5.1	<b>11</b> 40 ± 1.2	<b>18</b> 70 ± 6.2
	72-h	75 ± 6.6	50 ± 1.5	90 ± 5.5
2-Cl	24-h	25 ± 1.7	5 ± 0.8	10 ± 0.4
	48-h	60 ± 5.5	<b>13</b> 10 ± 0.6	<b>19</b> 30 ± 0.8
	72-h	80 ± 7.2	20 ± 0.8	45 ± 0.9
3-Cl	24-h	10 ± 0.9	15 ± 0.9	20 ± 0.2
	48-h	50 ± 3.7	<b>14</b> 20 ± 0.6	<b>20</b> 45 ± 1.1
	72-h	65 ± 5.9	45 ± 1.2	50 ± 1.2
4-Cl	24-h	50 ± 3.7	20 ± 0.5	10 ± 0.5
	48-h	60 ± 5.2	<b>15</b> 35 ± 0.8	<b>21</b> 30 ± 0.9
	72-h	80 ± 7.3	45 ± 1.4	45 ± 1.4
3,4-Cl <sub>2</sub>	24-h	5 ± 0.6	15 ± 0.8	20 ± 0.5
	48-h	45 ± 2.6	<b>16</b> 35 ± 1.5	<b>22</b> 30 ± 0.6
	72-h	65 ± 5.8	50 ± 1.8	50 ± 1.6

<sup>a</sup> Data for growth inhibition ratios taken from ref. [5].

Compounds were tested at a concentration of 50 µg mL<sup>-1</sup>.

Data (from five independent experiments) are shown as the mean ± standard deviation.

**Table 3**The IC<sub>50</sub> values for novel fused azaisocytosine-containing congeners (9-22).

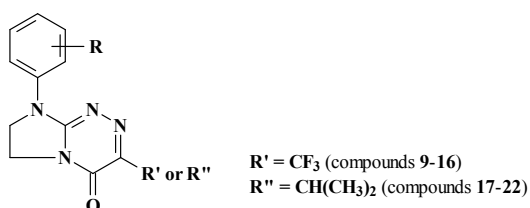
Compound	Incubation time	IC <sub>50</sub> values (mM)			
		Vero	A549	T47D	HeLa
<b>9</b>	24 h	> 0.18	> 0.18	> 0.18	> 0.18
	48 h	0.18 ± 0.003	> 0.18	0.11 ± 0.007	0.18 ± 0.006
	72 h	0.15 ± 0.003	0.18 ± 0.009	0.09 ± 0.006	0.11 ± 0.006
<b>10</b>	24 h	> 0.18	> 0.18	> 0.18	> 0.18
	48 h	> 0.18	> 0.18	0.11 ± 0.005	0.15 ± 0.007
	72 h	> 0.18	0.14 ± 0.004	0.09 ± 0.005	0.11 ± 0.006
<b>11</b>	24 h	> 0.18	> 0.18	> 0.18	> 0.18
	48 h	> 0.18	0.15 ± 0.007	0.11 ± 0.007	0.14 ± 0.008
	72 h	0.17 ± 0.005	0.11 ± 0.004	0.09 ± 0.005	0.10 ± 0.006
<b>12</b>	24 h	> 0.18	> 0.18	> 0.18	> 0.18
	48 h	> 0.18	0.14 ± 0.006	0.09 ± 0.005	0.18 ± 0.010
	72 h	> 0.18	0.10 ± 0.004	0.09 ± 0.005	0.09 ± 0.005
<b>13</b>	24 h	> 0.18	> 0.18	> 0.18	> 0.18
	48 h	> 0.18	> 0.18	0.11 ± 0.009	> 0.18
	72 h	> 0.18	0.12 ± 0.005	0.09 ± 0.003	0.11 ± 0.006
<b>14</b>	24 h	> 0.18	> 0.18	> 0.18	> 0.18
	48 h	> 0.18	0.13 ± 0.006	0.11 ± 0.008	0.18 ± 0.010
	72 h	0.18 ± 0.005	0.09 ± 0.005	0.09 ± 0.006	0.12 ± 0.006
<b>15</b>	24 h	> 0.18	> 0.18	> 0.18	> 0.18
	48 h	> 0.18	> 0.18	0.11 ± 0.006	0.13 ± 0.006
	72 h	0.18 ± 0.006	0.14 ± 0.006	0.09 ± 0.006	0.09 ± 0.005
<b>16</b>	24 h	> 0.18	> 0.18	> 0.18	> 0.18
	48 h	> 0.18	0.13 ± 0.007	0.09 ± 0.006	0.12 ± 0.005
	72 h	0.14 ± 0.005	0.09 ± 0.005	0.09 ± 0.007	0.09 ± 0.006
<b>17</b>	24 h	> 0.18	> 0.18	> 0.18	0.18 ± 0.005
	48 h	> 0.18	> 0.18	0.13 ± 0.010	0.13 ± 0.008
	72 h	0.18 ± 0.004	> 0.18	0.10 ± 0.003	0.10 ± 0.008
<b>18</b>	24 h	> 0.18	> 0.18	> 0.18	> 0.18
	48 h	0.13 ± 0.011	> 0.18	0.12 ± 0.005	0.13 ± 0.008
	72 h	0.10 ± 0.006	> 0.18	0.09 ± 0.005	0.10 ± 0.004
<b>19</b>	24 h	> 0.18	> 0.18	> 0.18	0.13 ± 0.009
	48 h	> 0.18	> 0.18	0.13 ± 0.005	0.10 ± 0.004
	72 h	> 0.18	0.14 ± 0.003	0.10 ± 0.005	0.09 ± 0.005
<b>20</b>	24 h	> 0.18	> 0.18	> 0.18	> 0.18
	48 h	> 0.18	> 0.18	0.14 ± 0.006	0.12 ± 0.006
	72 h	0.17 ± 0.004	0.17 ± 0.005	0.09 ± 0.004	0.10 ± 0.006
<b>21</b>	24 h	> 0.18	> 0.18	> 0.18	> 0.18
	48 h	> 0.18	> 0.18	0.14 ± 0.006	0.16 ± 0.010
	72 h	> 0.18	0.14 ± 0.005	0.09 ± 0.005	0.11 ± 0.005
<b>22</b>	24 h	> 0.18	> 0.18	> 0.18	> 0.18
	48 h	> 0.18	0.17 ± 0.006	0.10 ± 0.007	0.13 ± 0.006
	72 h	0.15 ± 0.005	0.13 ± 0.006	0.09 ± 0.006	0.10 ± 0.006
Standard drug	24 h	> 0.18	> 0.18	> 0.18	> 0.18
	48 h	> 0.18	> 0.18	> 0.18	0.18 ± 0.009
	72 h	> 0.18	0.18 ± 0.012	> 0.18	0.15 ± 0.011

The standard drug – pemetrexed

Data are shown as the mean ± standard deviation.

**Table 4**

Selectivity indices for all novel compounds.



R	Incubation time	Selectivity indices							
		A549		T47D		HeLa			
		R'	R''	R'	R''	R'	R''	R'	R''
H	24 h	~ 1.00	~ 1.00	~ 1.00	~ 1.00	~ 1.00	~ 1.00	~ 1.00	> 1.00
	48 h	<b>9</b> < 1.00	<b>17</b> ~ 1.00	<b>9</b> 1.64	<b>17</b> > 1.39	<b>9</b> 1.00	<b>17</b> > 1.39		
	72 h	0.83	< 1.00	1.67	1.80	1.36	1.80		
2-CH <sub>3</sub>	24 h	~ 1.00	~ 1.00	~ 1.00	~ 1.00	~ 1.00	~ 1.00	~ 1.00	~ 1.00
	48 h	<b>10</b> ~ 1.00	~ 1.00	<b>10</b> > 1.64	~ 1.00	<b>10</b> > 1.20	~ 1.00	~ 1.00	~ 1.00
	72 h	> 1.29	~ 1.00	> 2.00	~ 1.00	> 1.64	~ 1.00	~ 1.00	~ 1.00
4-CH <sub>3</sub>	24 h	~ 1.00	~ 1.00	~ 1.00	> 1.00	~ 1.00	> 1.00	~ 1.00	~ 1.00
	48 h	<b>11</b> > 1.20	<b>18</b> < 0.72	<b>11</b> > 1.64	<b>18</b> 1.08	<b>11</b> > 1.29	<b>18</b> 1.00	<b>11</b> > 1.29	<b>18</b> 1.00
	72 h	1.55	< 0.56	1.89	1.11	1.70	1.00	1.70	1.00
2-OCH <sub>3</sub>	24 h	~ 1.00	~ 1.00	~ 1.00	~ 1.00	~ 1.00	~ 1.00	~ 1.00	~ 1.00
	48 h	<b>12</b> > 1.29	~ 1.00	<b>12</b> > 2.00	~ 1.00	<b>12</b> > 1.00	~ 1.00	~ 1.00	~ 1.00
	72 h	> 1.80	~ 1.00	> 2.00	~ 1.00	> 2.00	~ 1.00	> 2.00	~ 1.00
2-Cl	24 h	~ 1.00	~ 1.00	~ 1.00	~ 1.00	~ 1.00	~ 1.00	~ 1.00	> 1.39
	48 h	<b>13</b> ~ 1.00	<b>19</b> ~ 1.00	<b>13</b> > 1.64	<b>19</b> > 1.39	<b>13</b> ~ 1.00	<b>19</b> > 1.80	<b>13</b> ~ 1.00	<b>19</b> > 1.80
	72 h	> 1.50	> 1.29	> 2.00	> 1.80	> 1.64	> 2.00	> 1.64	> 2.00
3-Cl	24 h	~ 1.00	~ 1.00	~ 1.00	~ 1.00	~ 1.00	~ 1.00	~ 1.00	~ 1.00
	48 h	<b>14</b> > 1.39	<b>20</b> ~ 1.00	<b>14</b> > 1.64	<b>20</b> > 1.29	<b>14</b> > 1.00	<b>20</b> > 1.50	<b>14</b> > 1.00	<b>20</b> > 1.50
	72 h	2.00	1.00	2.00	1.89	1.50	1.70	1.50	1.70
4-Cl	24 h	~ 1.00	~ 1.00	~ 1.00	~ 1.00	~ 1.00	~ 1.00	~ 1.00	~ 1.00
	48 h	<b>15</b> ~ 1.00	<b>21</b> ~ 1.00	<b>15</b> > 1.64	<b>21</b> > 1.29	<b>15</b> > 1.39	<b>21</b> > 1.13	<b>15</b> > 1.39	<b>21</b> > 1.13
	72 h	1.29	> 1.29	2.00	> 2.00	2.00	> 1.64	2.00	> 1.64
3,4-Cl <sub>2</sub>	24 h	~ 1.00	~ 1.00	~ 1.00	~ 1.00	~ 1.00	~ 1.00	~ 1.00	~ 1.00
	48 h	<b>16</b> > 1.39	<b>22</b> > 1.06	<b>16</b> > 2.00	<b>22</b> > 1.80	<b>16</b> > 1.50	<b>22</b> > 1.39	<b>16</b> > 1.50	<b>22</b> > 1.39
	72 h	1.56	1.15	1.56	1.67	1.56	1.50	1.56	1.50
Standard drug	24 h	~ 1.00	~ 1.00	~ 1.00	~ 1.00	~ 1.00	~ 1.00	~ 1.00	~ 1.00
	48 h	~ 1.00	~ 1.00	~ 1.00	~ 1.00	~ 1.00	~ 1.00	~ 1.00	~ 1.00
	72 h	> 1.00	~ 1.00	~ 1.00	~ 1.00	> 1.20	~ 1.00	> 1.20	~ 1.00

SI – selectivity indices are expressed as IC<sub>50</sub> of compounds in non-tumoural cells / IC<sub>50</sub> of compounds in cancer cell

The standard drug – pemetrexed

**Table 5**The effect of compound **12** on caspase-6 and -8 levels in normal and cancer cells

Cell line	Compound	Concentration (ng mL <sup>-1</sup> )	
		Caspase-6	Caspase-8
Vero	control	1.450 ± 0.4	0.816 ± 0.2
	<b>12</b>	1.746 ± 0.4	0.881 ± 0.4
A549	control	2.050 ± 0.5	0.767 ± 0.3
	<b>12</b>	3.020 ± 0.7*	0.909 ± 0.5*
T47D	control	1.526 ± 0.2	1.032 ± 0.5
	<b>12</b>	2.116 ± 0.3*	1.008 ± 0.6
HeLa	control	1.998 ± 0.4	0.698 ± 0.2
	<b>12</b>	2.342 ± 0.6	0.692 ± 0.3

Compound **12** was tested at a concentration of 50 µg mL<sup>-1</sup>.

Data (from three independent experiments) are shown as the mean ± standard deviation.

\* statistically significantly different from the control (p < 0.05, *t*-Student's test)

**Declaration of interests**

x The authors declare that they have no known competing financial interests or personal relationships that could have appeared to influence the work reported in this paper.

Journal Pre-proofs